Earth-Science Reviews 253 (2024) 104788

Contents lists available at ScienceDirect

Earth-Science Reviews

journal homepage: www.elsevier.com/locate/earscirev

A review and field guide for the standardized description and sampling of paleosols

Theresa J. Orr [a,*], Eric M. Roberts [a,b]

[a] College of Science and Engineering, James Cook University, QLD 4870, Australia
[b] Department of Geology and Geological Engineering, Colorado School of Mines, Golden, CO 80401, USA

ARTICLE INFO

Keywords:
Ancient soils
Pedogenesis
Paleoenvironment
Paleoclimate
Paleosol morphology

ABSTRACT

Paleosols are unrivaled terrestrial archives of paleoclimatic, paleoecological, and paleoenvironmental conditions, yet their full utility and potential for unlocking critical information about past ecosystems, as well as their comparability with other records, is dependent upon the quality and thoroughness of such studies. To help standardize communication and compatibility in and between paleopedology studies, a systematic review was conducted with the goal of providing a “field-guide” for helping investigators approach paleosol identification, description, classification. A paleosol logging sheet template was developed to help standardize field data collection and note taking, which includes a list of 30 items that should ideally be described. An accompanying sample log sheet was also developed to assist with collection of key data during the sampling phase of paleosol investigations. Based on this review, we conclude that examination of fresh surfaces focusing on horizonation, color, structure (peds), pedogenic features, mineral accumulations, and bioturbation (burrows/chambers and root traces) is critical to all paleosol investigations and standard field testing should include color of the paleosol matrix and mottles present, carbonate content, redoximorphic conditions, and presence of organic matter. To further facilitate this work, we have illustrated and tabulated key paleosol features and classification schemes, including horizon determination and classification; ped determination and classification; mottle description; mineral accumulation description/morphology; burrow/chamber morphology and description; and rhizolith morphology and classification. In addition, a review of best practices in the collection of samples for subsequent laboratory analyses and paleoenvironmental interpretations is presented.

1. Introduction

Paleosols are ancient or ‘fossil’ soils. These soils have been preserved in the stratigraphic record through burial or subsequent sedimentation events and may or may not be lithified (Tabor and Myers, 2015). Technically, a paleosol is any soil that has been buried by at least 50 cm of sediment, or by 30–50 cm if it constitutes at least half the total thickness of the paleosol (e.g., buried by 30 cm of sediment if the paleosol is ≤60 cm thick) (United States Natural Resources Conservation Service, 2014).

Paleosols are preserved throughout carbonate, clastic and volcanic strata, on all continents, and throughout geologic time. Indeed, the oldest interpreted paleosols date back >3 billion years to the Archean (Retallack, 2018; Retallack and Noffke, 2019). Soil formation is controlled by the five soil forming factors, biota (organisms), climate, parent material, time, and topography. Anthropogenic activity is also an integral factor in the formation of modern soils (Yaalon and Yaron, 1966), but it has little, if any relevance in the study of paleosols. It is the process of soil formation in response to the key controlling factors that make paleosols such valuable archives of climate and environmental data. Soils form over tens of thousands (or even millions) of years (Retallack, 1983), capturing information about the average conditions throughout the period of formation. Although changes in the climate and environment can also be preserved (e.g., vertical and lateral changes in a paleosol’s morphology and composition). These time capsules of paleoclimate and paleoenvironment information are found in natural exposures (e.g., outcrops, river channels) or can be discovered in pits and sediment cores (e.g., Kraus, 1999; Retallack, 2001) (Fig. 1).

This guide reviews and describes various field techniques that can be used for 1) preliminary paleosol description and classification, 2) gathering of information for subsequent paleoenvironment interpretations and 3) collection of samples for laboratory analyses.

* Corresponding author.
E-mail address: theresa.orr@my.jcu.edu.au (T.J. Orr).

https://doi.org/10.1016/j.earscirev.2024.104788
Received 8 November 2023; Received in revised form 20 April 2024; Accepted 22 April 2024
Available online 24 April 2024

Several guides exist for the recognition and description of paleosols (e.g., Retallack, 1988; Mack et al., 1993; Tabor et al., 2017); however, there remains a need for detailed sampling instructions and logging protocols to improve comparability in and between studies, and to ensure the collection and generation of usable and publishable data. This is particularly true when paleoclimate and paleoenvironment reconstruction is the primary aim of a study. This beginners guide has been created to serve sedimentologists, paleontologists, geomorphologists, and other researchers, and is intended to assist in the following, 1) detailed investigations for the description and classification of paleosols, and 2) field collection of information and samples required for paleoclimate and paleoenvironment reconstruction.

The complex nature of biological, chemical, and physical interactions in a soil indicates the use of multiple proxies are needed to capture an accurate overview of the paleoclimate and paleoenvironment under which the soil formed (e.g., Kraus, 1999, Driese et al., 2000, Retallack, 2001, Sheldon and Tabor, 2009, Nordt and Driese, 2010, Tabor and Myers, 2015). Appropriate collection of field data and samples can help identify the different atmospheric, climatic and environmental conditions during soil formation. Macromorphological data is particularly useful for determining sedimentation regimes, pedogenic processes, soil and landscape types, paleosol maturity, soil drainage characteristics, and broad paleoclimatic conditions (e.g., wet vs dry) (Tabor and Myers, 2015). In tandem with this, ichnological data on root- and burrow- traces provide direct evidence of the flora and fauna that the soil supported before it was buried. Using models and/or climofunctions, geochemical data provides for a more quantitative reconstruction of the paleoclimate. Major element geochemistry can be used

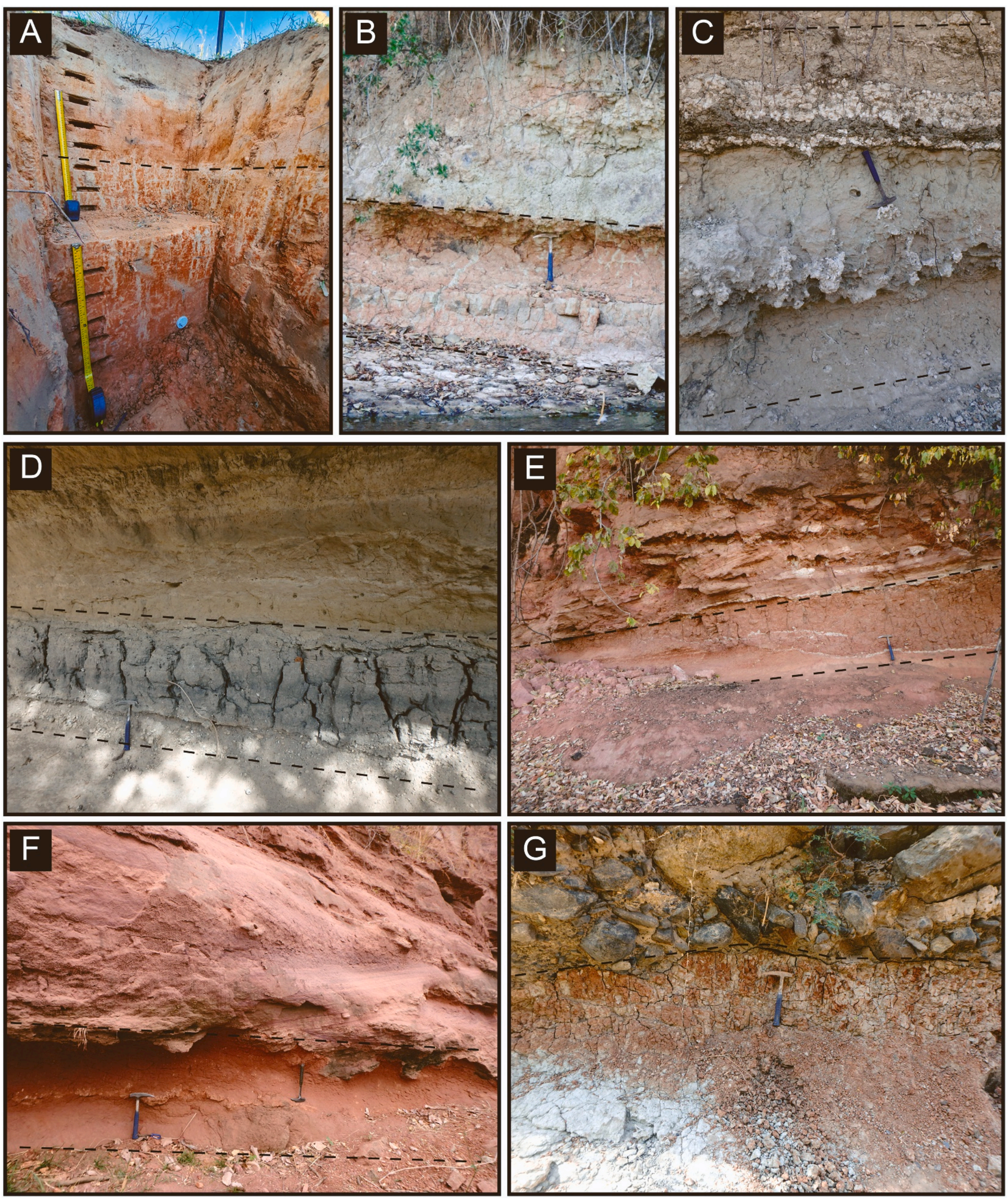

Fig. 1. Paleosol profiles at the outcrop scale: A) Pleistocene paleosol in a fresh pit under a modern dune in central Northern Australia; B) Oligocene paleosols exposed in recent river cut in the Rukwa Rift Basin (RRB), Tanzania; C) clay-rich Miocene paleosol in a river cut in the RRB, Tanzania; D) Holocene pumice-paleosol in a recent river cut, in the RRB, Tanzania; E) – F) Cretaceous red paleosols in a recent river cut in the RRB, Tanzania; G) Oligocene paleosol in a recent river cut in southwest Tanzania. Dashed lines: upper and lower profile boundary. Scale in Parts B-G is a rock hammer 33 cm long. (For interpretation of the references to color in this figure legend, the reader is referred to the web version of this article.)

to determine mean annual precipitation and temperature values, as well as humidity regimes, and the dominant pedogenic or weathering processes (Tabor and Myers, 2015). The stable isotope composition of mineral accumulations can be used to estimate the atmospheric concentration of CO_2, generate meteoric water lines, and identify hydrologic changes (e.g., Khademi et al., 1997; Ludvigson et al., 2013; Orr et al., 2022). When combined, these data enable us to develop the natural history of our planet, provide context to known fossil assemblages, and help us to better understand evolutionary drivers and landscape shifts in the face of climate and environmental change.

2. Field methods and equipment

2.1. Field description

A paleosol is typically identified from the surrounding strata by the presence of soil horizons and structure (peds), and evidence of bioturbation in the form of root traces and/or burrows (Retallack, 1988). Root convergence or truncation can often be seen at the top of a profile, depending on whether the profile has an upper erosional surface or if the upper horizons (O and A) have been preserved (e.g., Gürel, 2017). A paleosol should only be described from a fresh surface; therefore, depending on the exposure of the profile some digging may be required. For example, a paleosol being described from a fresh pit or core will not require any further extraction; however, those profiles naturally exposed in outcrop will likely require at least 20 cm removed to access a fresh surface, and in some cases 50+ cm may be required.

Multiple profile and pedogenic features exist in a single paleosol unit that require detailed description. These features vary laterally, and the collection of several profile descriptions at various lateral exposures can help identify pedofacies and, subsequently, interpret the paleoenvironment (Kraus, 1999). The feasibility of collecting such data is limited by the nature of the paleosol exposure. Pit and core exposures are generally limited to a single profile description, although multiple pits and cores may be taken to capture spatial variation. Natural exposures, such as river cuttings, allow for the comparably easy description of many profiles. The number of profiles described will also depend on the scale of the individual study. Local-scale landscape associations can be determined from paleosol data captured over a few meters to kilometers (e.g., <2 km), with basinal-scale associations determined from data collected over tens (or even hundreds) of kilometers (e.g., Kraus, 1999). Table 1 summarizes the key paleosol features that should be described to ensure paleoclimatic and paleoenvironmental conditions can be modelled using geochemical or morphological techniques later.

In general, paleosols represent periods of landscape stability, preserving the degree of soil development or maturity attained prior to burial (Marriott and Wright, 1993; Kraus, 1999). Pedogenesis uninterrupted by periods of erosion or sedimentation forms simple profiles that become increasingly mature, and usually exhibit clear horizonation. A simple profile can become overprinted by a new profile if climatic or environmental conditions sufficiently alter, forming a polygenetic profile. However, active periods of sedimentation can be documented by the generation of several soil profiles within a single paleosol (Marriott and Wright, 1993). Composite and compound profiles are influenced by rapid, episodic sedimentation. Short-lived or small depositional events form composite paleosols, which are characterized by overlapping profiles, A-B horizon overprinting and weak development. Whereas longer or larger depositional events form compound paleosols, with profiles separated by the sediment deposit. Cumulate profiles form under steady sedimentation conditions; deposition consists of small increments and the rate of pedogenesis withstands the rate of aggradation by overprinting lower horizons (Marriott and Wright, 1993). These profiles are characterized by a thick profile and B-B horizon overprinting is common. Multiple sedimentation regimes can be documented in a profile's vertical section (Fig. 2), with morphology and maturity laterally varying with proximity to primary sedimentation environments e.g., fluvial channels (Kraus, 1999). Where erosional events are recorded in a profile, the term 'truncated' is used as a prefix-modifier for profile designations (Kraus, 1999).

Paleosol classification is usually conducted in the field, and aids in the collection of appropriate data and samples. Several classification schemes exist for modern soils (e.g., United States (US) Soil Taxonomy (United States Natural Resources Conservation, 1999); however, the only classification scheme recommended for paleosol classification is that of Mack et al. (1993) (Fig. 3; Table 2). The classification scheme is based on parameters and pedogenic features that are preserved in the stratigraphic record, and readily available for assessment whilst in the field (Mack et al., 1993). A paleosol is classified according to its most prominent feature, and where multiple significant features are apparent subordinate (prefix) modifiers are used (Table 3) (Mack et al., 1993). Once classified a paleosol may then be compared to their modern equivalents for additional climatic and environmental interpretations (Retallack, 1998). Histosols, Oxisols, Spodosols and Vertisols may all be directly compared using the US Soil Taxonomy. An Argillisol is recognized by its subsurface illuvial clay horizon, with low-base (dystric) and high-base (eutric) Argillisols comparable to Ultisols and Alfisols, respectively. Depending on the maturity of a Protosol's horizons, it may be compared to an Entisol (less developed) or Inceptisol (more developed). The concept of Calcisols and Gypsisols is present in the US Soil Taxonomy but not as a great order, although they do have some similitude with Aridisols. Gleysols are also not present as a great order, but generally correlate with the Aqu suborder. Paleosol classifications can also be used to determine the pedotypes or paleosol series in a given area (Retallack, 1994).

Table 1
Recommended paleosol features for description in the field.

Feature	Relevant section	Sample required	Applicable methods
Color	2.2	×	Morphology
Horizon (matrix)	3.1	✓	Geochemistry Mineralogy Morphology Petrography
Structure	3.2	×	Morphology
Pedogenic features	3.3	✓	Morphology Petrography
Mineral accumulations	3.4	✓	Geochemistry Mineralogy Morphology Petrography
Burrows and chambers	3.5	×	Ichnology Morphology
Root traces	3.6	✓	Geochronology Morphology

2.2. Field testing

A number of useful tests can be conducted that will assist in the analysis of a paleosol. The results of these tests are typically qualitative but are informative. The primary tests include 1) color, 2) carbonate content (or calcareousness), 3) redoximorphic conditions, and the presence of 4) organic matter, 5) gypsum or 6) evaporative soluble salts. Many of these protocols are optional and will depend on the specific study and soil type, but documenting the color of the paleosol matrix is essential. These tests are in addition to standard sedimentological data that should be collected pro forma (e.g., grain size, sorting, rounding, composition).

It is important to recognize that paleosols and modern soils are distinctly different. Testing for modern soil parameters, such as pH or EC, is generally redundant in paleosols as many of these parameters are altered during burial, compaction, and lithification processes, and can no longer be used to interpret the soil environment (Mack et al., 1993).

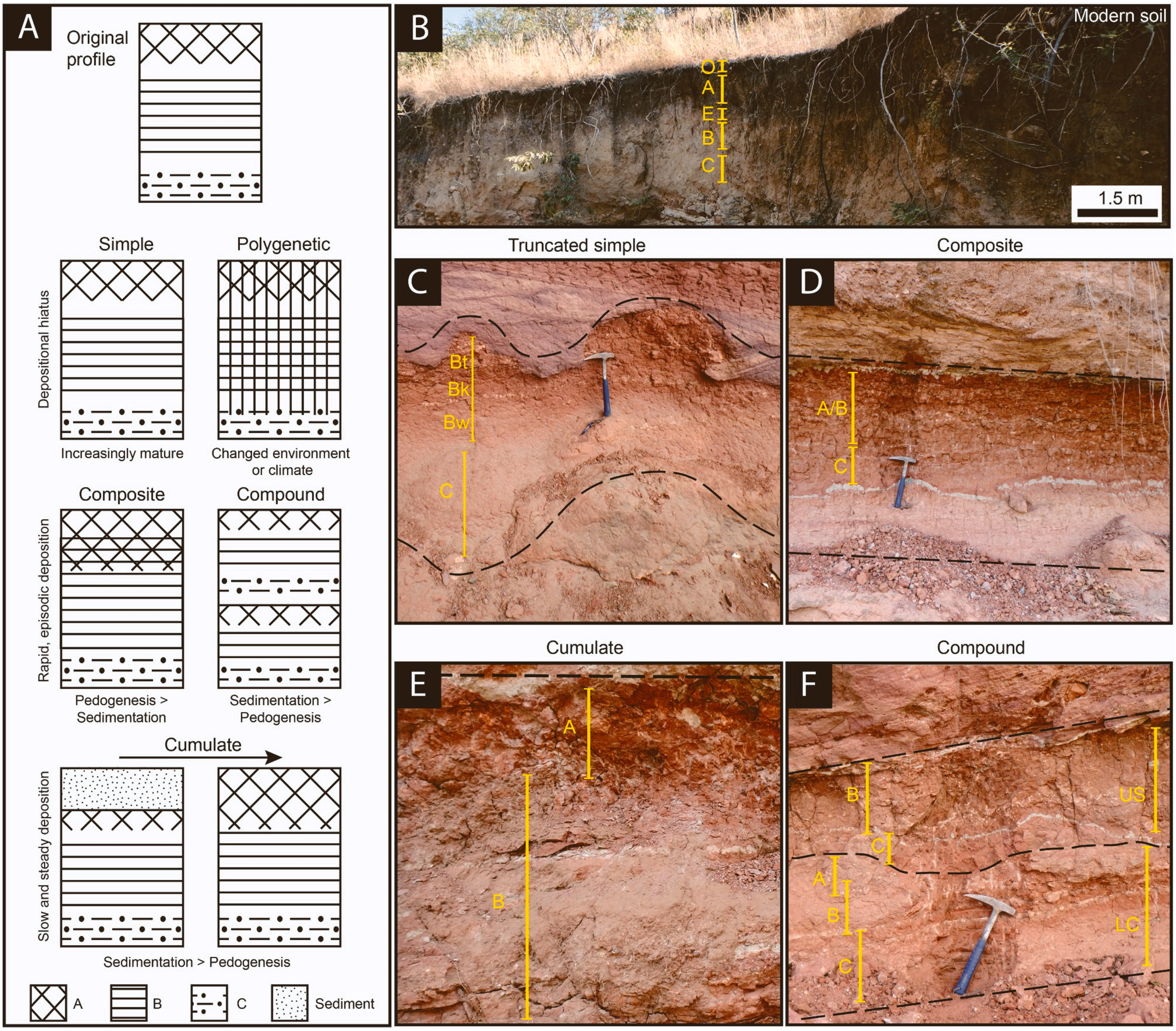

Fig. 2. Examples of modern soil and paleosol profiles with horizon designations: A) schematic diagram showing the paleosol profiles that form under varying rates of sedimentation and pedogenesis; B) Modern soil profile; C) truncated simple; D) composite profile with overprinted A/B horizons; E) cumulate profile with thick B horizon; F) compound with an upper simple (US) and lower composite (LC) profile, identified by repeated B-C profile. Dashed lines: upper and lower profile boundary. Scale in C-F is a rock hammer 33 cm long.

The most obvious visual difference is the general absence of O and A horizons in the paleosol record. Erosional upper surfaces are the norm, and the removal of the uppermost horizons signifies the loss of soil with the greatest biological activity and climate interaction. There are additional differences between modern soils and paleosols that highlight the mineralogical and geochemical changes engendered by diagenesis and lithification. For example, the colloidal fraction of a soil can be altered (Tabor and Myers, 2015) or Fe can be diagenetically removed from a profile and can be difficult to differentiate from pedogenic losses (Maynard, 1992). For this reason, pedogenic features that survive diagenesis and lithification form the basis of paleosol description and classification, with several identified through the tests provided here.

2.2.1. *Color*

The color of the paleosol matrix, and typically any mottles that are present, is determined using a Munsell Soil-Color Charts book (Munsell, 2009). The hue and chroma of the colors assist in identifying areas of redox or waterlogging within the profile, and provides clues to the mineral content (Retallack, 1988, 1998). Blue, grey or green colors of generally low chroma values (<2) typically indicate redox depletions, whereas red, purple and yellow hues may represent areas of redox concentration and mineral accumulations (e.g., Fe-oxides), especially when bordering zones of depletion (e.g., Vepraskas, 2004; Kraus and Hasiotis, 2006; Tabor and Myers, 2015). There are exceptions, 1) the color of paleosols with organic matter accumulations, low chroma and color values ≤ 3 is associated with the organic content, rather than redox conditions and 2) low chroma colors resulting from low-Fe parent materials (Vepraskas, 2004). Color is determined from a fresh surface within a few minutes of exposure to avoid oxidation-related color changes, with the sample either dry or moist. Moist is recommended as it is impossible to know how dry a sample is. However, wetting is easily done prior to recording the color and facilitates the collection of consistent data. The sample may be moistened using a small spray or squeeze bottle, with (preferably) distilled water. Color determinations can be made once a sample's color no longer changes with additional wetting; however, glistening surfaces should be avoided as the light reflection can lead to erroneous color designations (Munsell, 2009).

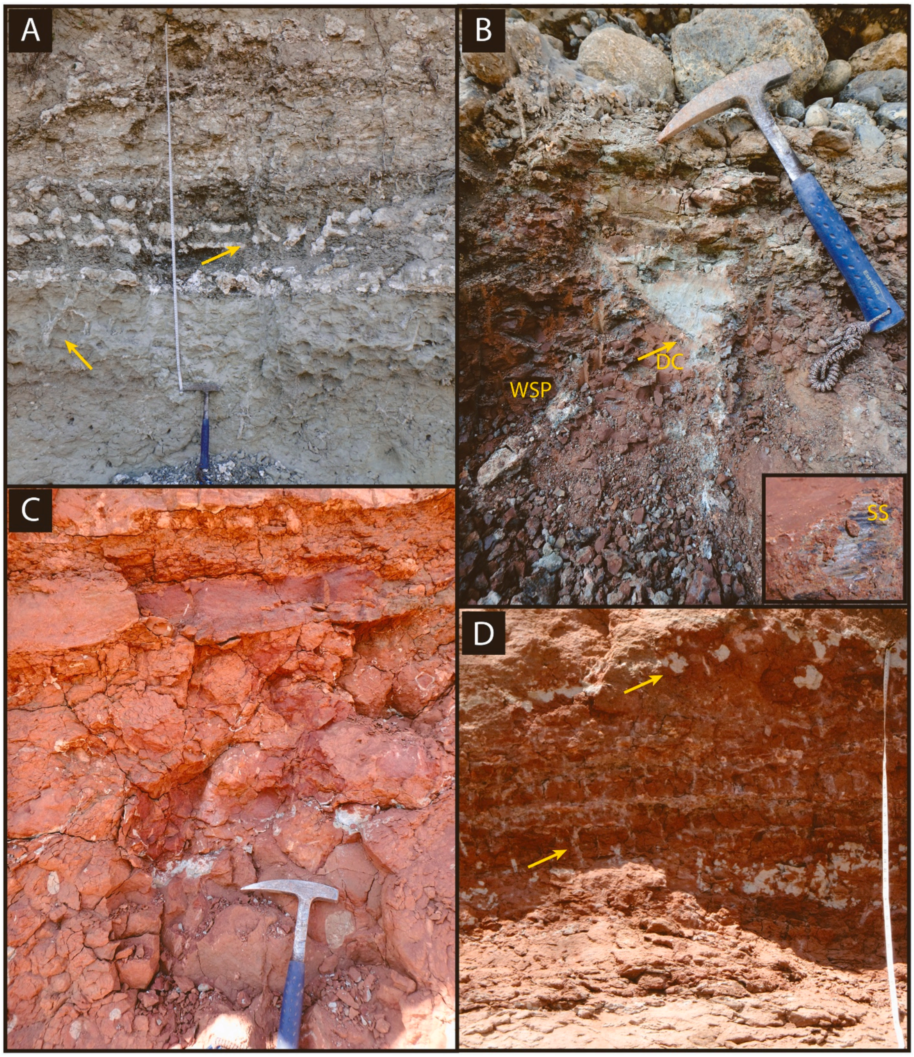

Fig. 3. Examples of paleosol order classifications: A) argillic Calcisol from the Miocene, RRB Tanzania, with extensive burrow networks and distinct carbonate accumulations as indicated by the yellow arrows; B) A and B horizon of an Oligocene Vertisol from the RRB, Tanzania, with sediment-infilled desiccation crack (DC), wedge-shaped peds (WSP), and slickenside (SS; inset); C) argillic Protosol from the Cretaceous, RRB Tanzania, displaying weak ped development and horizonation; D) Cretaceous calcic Argillisol from the RRB, Tanzania, with bleached upper boundary and abundant root mottles (rhizohaloes) as indicated by the yellow arrows. Scale is a rock hammer 33 cm long. (For interpretation of the references to color in this figure legend, the reader is referred to the web version of this article.)

2.2.2. Carbonate content

Carbonate content is determined by applying dilute HCl acid (~10%) to the paleosol matrix, and or accumulations (Retallack, 1988). A small acid dropper bottle can be used to apply a few drops to freshly exposed surfaces. Where necessary the samples may be crushed beforehand to better expose (and differentiate the reaction between) the matrix and mineral accumulations. The carbonate content classification has five levels (Retallack, 1988). Where no reaction is observed the sample is considered noncalcareous, with the acid often forming an inert bead. Very weakly calcareous samples exhibit little movement *within* the acid drop, whereas numerous bubbles that do not coalesce indicate a calcareous content. Bubbles that form a white froth are designated strongly calcareous, and very strongly calcareous once the frothing becomes vigorous and demonstrates some doming upwards. The calcareousness of the substrate is an indicator of base saturation (Retallack, 1988).

2.2.3. Redoximorphic conditions

The presence of reduced iron, as an indication of redoximorphic conditions, may be determined by applying a neutral (pH 7) 0.2% solution of α,α'-dipyridyl dye dissolved in 1 N ammonium acetate (Vepraskas, 2004). The solution is prepared by dissolving 77 g of ammonium acetate in 1 L of distilled water, before adding 2 g of α,ά-dipyridyl powder and stirring until dissolved. The colorless solution must be prepared in advance and stored in the dark until use, because it is sensitive to light (Vepraskas, 2004). The solution should then be sprayed onto a moist fresh sample. If ferrous iron is present, a pink color will appear within a few minutes (Vepraskas, 2004). It is important to note that while this test has been used for modern soils (e.g., Martindale et al., 2019), it has not yet been applied extensively to paleosols and the efficacy of its results for ancient soils is unknown. However, the presence of ferrous iron may be confirmed later in the laboratory for comparison via potentiometric titration (e.g., Goldich, 1984; Babechuk and Kamber, 2013; Orr et al., 2023).

2.2.4. Organic matter

Organic matter is typically identified by dark grey or black colors in the upper horizons of a profile. However, application of dilute hydrogen peroxide can discern organic matter from manganese oxides. A 5% solution of hydrogen peroxide is applied to the bulk matrix, the presence of organic matter is confirmed when the reaction starts slowly but builds and continues to produce bubbles (United States Department of

Table 2
Paleosol order classification, based on the prominent pedogenic features of a profile. Data sourced from Mack et al. (1993).

Paleosol order	Prominent feature
Argillisol	Subsurface horizon containing illuvial clay (argillic horizon) *Refer to section 3.3 and Table 8 for argillic morphologies*
Calcisol	Pedogenic calcic horizon *Refer to section 3.4 and Table 11 for carbonate morphologies*
Gleysol	Evidence of persistently low redox conditions (e.g., low chroma colors, carbonaceous material, pyrite) May be surface or subsurface horizon Mottled horizon may be present
Gypsisol	Pedogenic gypsum or anhydrite horizon May be surface or subsurface horizon *Refer to section 3.4 and Table 11 for gypsum morphologies of vadose origin*
Histosol	Coal or peat horizon present (regardless of thickness)
Oxisol	Extensive alteration of chemically unstable minerals to clay and/or sesquioxides in situ (<10% unstable grains remain) Oxic horizon was a subsurface horizon
Protosol	Weak horizonation (unrelated to homogenization by pedoturbation)
Spodosol	Subsurface illuviation of organic matter and iron oxides
Vertisol	Homogenization of profile by pedoturbation *Refer to section 3.3 for vertic morphologies*

Table 3
Subordinate modifiers for paleosol orders. Data sourced from Mack et al. (1993).

Subordinate modifier	Prominent feature
Albic	Eluvial horizon
Allophanic	Allophane or other amorphous Si and Al compounds
Argillic	Illuvial clay
Calcic	Pedogenic carbonate
Carbonaceous	Organic-rich that is not coal
Concretionary	Spherical nodules with concentric fabric
Dystric	Low base status (scarcity of unstable grains e.g., feldspars)
Eutric	High base status (abundance of unstable grains e.g., feldspars)
Ferric	Iron oxides
Fragic	Subsurface horizon that was hard during soil formation
Gleyed	Evidence of waterlogging
Gypsic	Vadose gypsum or anhydrite
Nodular	Glaebules with undifferentiated internal fabric
Ochric	Light colored horizon (commonly grey; Moist Munsell chroma ≥3/5)
Salic	Pedogenic salts (more soluble than gypsum)
Silicic	Pedogenic silica
Vertic	Vertic morphological features (*refer to section 3.3*)
Vitric	Relict (or actual) glass or pumice particles

Agriculture, 1971). Whereas a rapid production of bubbles and consumption of the hydrogen peroxide solution will occur in the presence of manganese oxides (United States Department of Agriculture, 1971). The applicability of this test depends on the age of the paleosol. Paleosols have less organic matter than modern soils with this differentiation increasing with time since burial, in part because of burial decomposition and/or diagenesis (Broz, 2020). The nature and composition of organic matter preserved in paleosols has also changed throughout geologic time, for example Precambrian paleosols that predate the evolution of plants (Broz, 2020). Application of hydrogen pyroxide is most appropriate for paleosols with colors that indicate the presence of organic matter accumulations and are of relatively young age (viz. Cenozoic), and those that exhibit evidence of waterlogging, such as Histosols, that extend to the Permian, as these paleosols still show enrichment in organic carbon (e.g., Krull and Retallack, 2000; Metzger and Retallack, 2010; Gulbranson et al., 2022).

2.2.5. Gypsum

The presence of gypsum is determined by heating a sample of the grains in question. Anhydrite and hemihydrate will normally appear chalky white; however, colorless gypsum crystals will turn white upon heating. This test is usually conducted by heating a small sample on a metal plate (Shearman, 1979). Individual gypsum grains may be hand-picked, or a teaspoon of sand-sized sediment may be used after removing any silt and clay. This method is applicable to siliciclastic sediments, but can also be used for carbonates, with the white color of the heated gypsum more intense than that of the carbonate (Shearman, 1979).

2.2.6. Salts

The presence of potassium and sodium chloride or nitrate, and sulfate salts, such as halite, is verified by mixing a small sample of crystals with ~10 mL of (preferably) distilled water. These salts are water-soluble and should dissolve. The crystal grains should also not react to dilute HCl and, where safe to do so, may be checked for a saline taste (United States Department of Agriculture, 1971).

2.3. Field logging and sampling sheets

Form 1 (Appendix A) is a logging sheet of 30 items that should ideally be described in the field. Many of these required items have specific morphologies or features that should also be noted. Each of these paleosol or pedogenic features are detailed in sections 3.1 to 3.6, with the provision of any applicable sub-classification schemes to assist in field note taking. The primary categories include paleosol horizon, structure, mineral accumulations, and pedogenic and bioturbation features. The form contains columns for describing each pedogenic feature, including type, color, dimensions and abundance, with rows available for each horizon. Space is also provided for general comments under each pedogenic feature. Form 2 (Appendix B) is a checklist for sample collection; it contains columns for the paleosol ID, sample number and sample type.

3. Field description

Paleosol pedogenic and bioturbation features, and mineral accumulations reflect the average climatic and environmental conditions during soil formation (Tabor and Myers, 2015). In describing these features, a near complete picture of the paleoclimate, paleoecology and paleoenvironment can be constructed. The description procedure for each category is simple and requires minimal field equipment. Where possible, the climatic, environmental, faunal, and floral associations have been provided here for context.

3.1. Horizons

Soils comprise a series of morphologically differentiated, vertically adjacent layers that reflect soil-forming processes, and ultimately the paleoenvironment and paleoclimate conditions under which they formed (CSIRO, 2009). These layers are classified as either master or transitional horizons and are assigned capital letters (United States Natural Resources Conservation, 1999). A modern soil profile will often have O, A, E, B, C and R horizons (Fig. 4). O and A horizons are dark surface layers primarily composed of organic material with a minor mineral component. A horizons contain less organic matter than O horizons and are the top mineral soil horizon. E horizons contain little clay or organic material as they are a zone of intense leaching (eluviation). B horizons are zones of illuviation, where the material that has eluviated from the overlying A and/or E horizons accumulates. C horizons contain partially weathered material with very little pedogenic alteration, whereas R horizons are consolidated bedrock. However, modern soil taxonomy identifies a large array of horizons that are not entirely applicable to paleosols (Mack et al., 1993). Paleosols are frequently

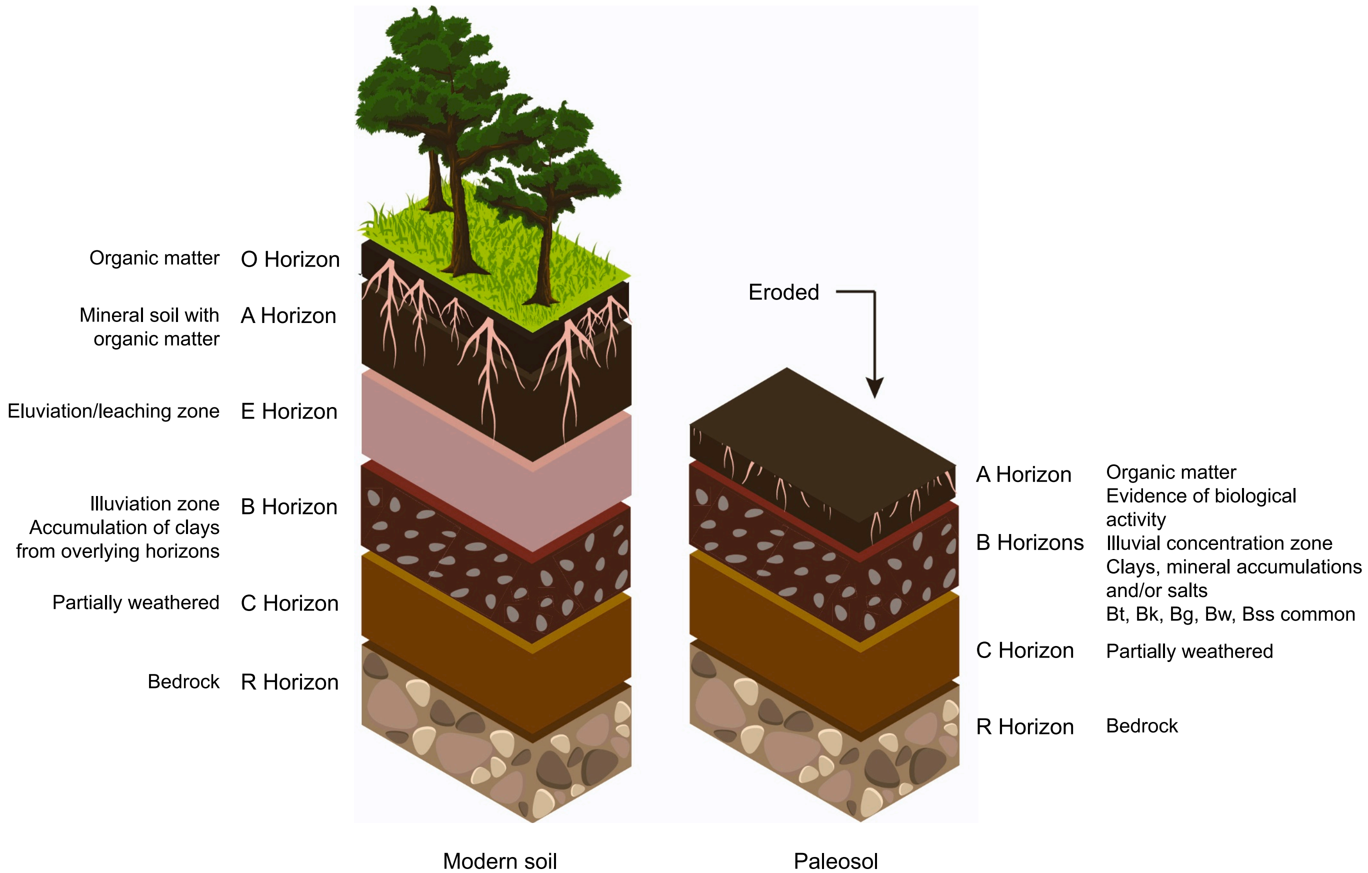

Fig. 4. Idealized modern soil profile and a simple paleosol profile modified after the US Soil taxonomy (United States Natural Resources Conservation, 1999). The upper horizons common in modern soils are often not preserved in paleosols because they are removed by erosion.

truncated, with their upper horizons removed, yet multiple B horizons are commonly preserved, a reflection of long periods of pedogenesis, and changes in sedimentation regimes or climatic conditions during soil formation (Tabor and Myers, 2015). Many paleosols will exhibit A-B-C or B-C profiles (Fig. 4), with the top O and A layers partially or wholly eroded; however, more complete profiles may be preserved in aggradational sedimentary basins or in volcanic areas where they are rapidly buried by deposition (e.g., Demko et al., 2004; Beverly et al., 2017). Mineral soil horizon designation and descriptors are generally consistent between the different modern soil and paleosol taxonomies and are easily recognizable in the literature. Table 4 provides the features characteristic of each horizon typically found in paleosols, with subordinate descriptors provided in Table 5. The reader is directed to the US Soil Taxonomy (United States Natural Resources Conservation, 1999) for the complete master and transitional horizon designations and subordinate descriptors.

Subordinate modifiers are particularly important as they are diagnostic in the paleosol order taxonomic classification of Mack et al. (1993). This is especially true in relation to B horizons, which frequently represent the most prominent feature of a paleosol. B horizons are also typically the most abundant horizons in a paleosol profile; however, only a few types are common in the rock record (Tabor et al., 2017). Of particular note are the Bg, Bk, Bss, and Bt horizons.

Once each horizon has been identified it is important to record the sharpness and morphology of the vertical transitions between the horizons, and the lateral continuity of the boundaries (Fig. 5; Table 6; Retallack, 1988). Boundary morphology only needs to be recorded for either the upper or lower bounding surface, with overlying horizons capturing the next boundary. Description of the upper boundary for each horizon is recommended as this captures the transition to the overlying unit. In paleosols that exhibit weak horizonation, such as Protosols, the profile's upper- and lower-unit boundary may be the only transitions visible for documentation. The abruptness of horizon transitions and the smoothness of the lateral continuity provides insight into the pedogenic processes at play throughout the period of soil formation (Kraus, 1999). Most importantly, the extent of deposition, erosion or polygenesis can be reviewed in relation to the profile classification scheme of Marriott and Wright (1993).

3.2. *Structure*

The basic structural unit of a paleosol (and modern soil) is the ped. Peds are the product of pedogenic processes, including the shrinking and swelling of clays, bioturbation, and cracking around roots and burrows (Retallack, 1988). Soil structure is an integral component of paleosol-derived paleoenvironmental reconstructions because ped morphology is the direct result of the dominant formational processes, as modulated by environmental and climatic conditions (Retallack, 1988). Peds are often visible in the exposed profiles of unlithified paleosols, but in many lithified paleosols the material must be broken apart to observe these single structural units (rather than larger structural aggregates) (Tabor et al., 2017). Many peds will have clay coatings, mineral accumulations, or slickensides on their planes, that are absent from larger aggregates. Peds are described in terms of shape and size, with changes down profile through the horizons also documented. Table 7 contains the applicable ped-structure classification scheme, related morphology and pedogenic process associations. The classification terminology follows that of United States Department of Agriculture (1975) but there are modified versions by Retallack (1988) and Birkeland (1999) more relevant to paleosols.

Peds are preserved in most paleosols despite burial and/or lithification processes, although some types are more common than others.

Table 4
Recognition criteria for paleosol horizon designation modified from the US Soil Taxonomy (United States Natural Resources Conservation, 1999) and Australian Soil and Land Survey Field Handbook (CSIRO, 2009).

Horizon designation	Master / transitional	Descriptor
A	Master	Mineral horizon that formed near or at surface May have organic matter Maximum biologic activity of the profile Morphology distinct from underlying horizons
B	Master	Mineral horizon that formed below an A, E or O horizon Obliteration of parent material structure Illuvial concentration of clay, iron, aluminium, sesquioxides, carbonates, humus, anhydrite, gypsum, other salts, or silica Different structure &/or consistence &/or stronger colors than A horizon or any horizon immediately below
C	Master	Mineral horizons that are consolidated or unconsolidated partially weathered material Weak modification by pedogenic processes
R	Master	Continuous mass of strongly cemented to indurated bedrock May have cracks but are too few/fine for roots to penetrate
AB / BA	Transitional	Horizon dominated by properties of either the A or B horizon, but with subordinate properties of the other horizon. AB – more characteristic of the A horizon than the B horizon BA – more characteristic of the B horizon than the A horizon
BC / CB	Transitional	Horizon dominated by properties of either the B or C horizon, but with subordinate properties of the other horizon. BC – more characteristic of the B horizon than the C horizon CB – more characteristic of the C horizon than the B horizon

Table 5
Recognition criteria for common paleosol subordinate modifiers, modified from the US Soil Taxonomy (United States Natural Resources Conservation, 1999).

Suffix symbol	Descriptor
c	Accumulation of concretions or nodules of Fe, Al, Mn or Ti (Anhydrite, calcite, gypsum, dolomite, silica or soluble salt accumulations are not included in this subordinate modifier)
g	Gleying (greyish, bluish or green colors of generally low chroma)
h	Illuvial accumulation of amorphous complexes of organic matter and sesquioxides where Al > Fe
j	Accumulation of jarosite
k	Accumulation of secondary carbonates. Typically present as filaments, coatings, masses or nodules.
m	Pedogenic cementation, >90% of horizon with strong cementation (irreversible) or induration (may be fractured)
q	Accumulation of secondary silica
r	Weathered or soft bedrock
s	Illuvial accumulation of amorphous complexes of organic matter and sesquioxides where Fe > Al
ss	Presence of pedogenic slickensides
t	Accumulation of silicate clay
w	Development of color &/or structure with little to no illuvial accumulation of material Applicable to B horizons only
x	Fragipan (high bulk density horizon relative to adjacent layers)
y	Accumulation of gypsum
z	Accumulation of salts more soluble than gypsum

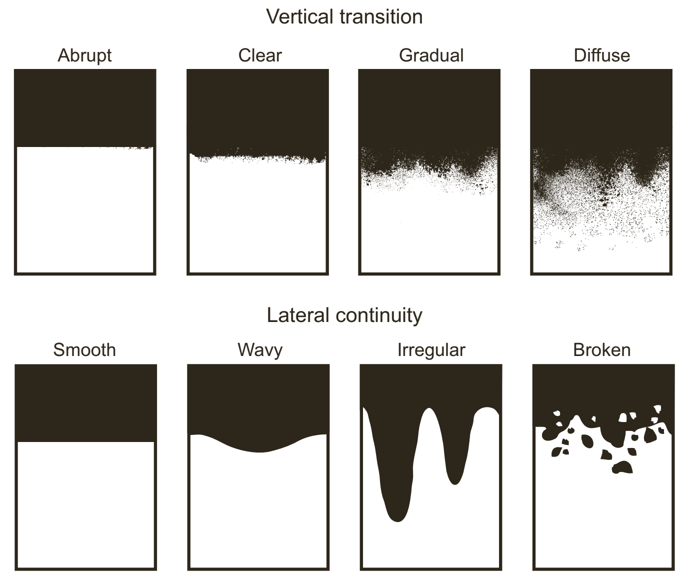

Fig. 5. Schematic diagram of horizon boundary morphologies, including vertical transition and lateral continuity. Four levels are identified in each category: abrupt, clear, gradual, and diffuse are used to describe the vertical transition between a horizon and the overlying layer, whereas smooth, wavy, irregular, and broken describe the lateral continuity of the individual horizon. The uppermost boundary morphology is noted for a horizon with additional horizons capturing the next boundary.

Table 6
Field description criteria for horizon boundaries. Data sourced from Retallack (1988) and CSIRO (2009).

Form	Descriptor	Morphology
Vertical transition (Boundary Sharpness)	Abrupt	Transition from one horizon to another is <1″ (<2 cm)
	Clear	Transition from one horizon to another is 1–2.5″ (2–5 cm)
	Gradual	Transition spread over 2.5–5″ (5–15 cm)
	Diffuse	One horizon grading into another over >5″ (>15 cm)
Boundary lateral continuity	Smooth	Horizon boundary forms an even plane (planar) Often parallel with master bedding planes
	Wavy	Horizon boundary undulates (sinusoidal) Wavelengths wider than deep
	Irregular	Horizon boundary undulates (sinusoidal) Wavelengths deeper than wide
	Broken	Parts of adjacent horizon are disconnected Some mixing of underlying and overlying horizon components (due to erosion or pedogenesis)

Prismatic and columnar peds are not commonly observed in paleosols. Whereas angular to subangular blocky, and wedge-shaped peds are the most frequently observed peds in the stratigraphic record (Tabor et al., 2017) and are characteristic of B horizons (Mohammed et al., 2020). Whereas granular peds are the dominant ped class found in surface horizons (A horizons) (Mohammed et al., 2020), but are often removed by erosion and rarely preserved in paleosol profiles (Tabor and Myers, 2015). Granular and crumb peds are also subject to modification during compaction (Mack et al., 1993) and are, thus, infrequently preserved. Comparatively, prismatic, columnar, and platy peds are infrequently observed even in modern soils (Mohammed et al., 2020). Fig. 6 is a schematic diagram of the different ped classes, whereas Fig. 7 highlights some of the more commonly observed ped structures in paleosols. The size of peds typically increases down-profile in response to a decrease in the intensity of pedogenic processes (Schaetzl and Thompson, 2015).

Table 7
Ped classification according to size and shape, and the relevant pedogenic processes. Data sourced from United States Department of Agriculture (1975), Retallack (1988), Birkeland (1999).

Ped	Morphology	Size	Size class	Pedogenic process
Angular blocky	Equant to rectangular Sharp interlocking edges	<0.5 cm 0.5–1 cm 1–2 cm 2–5 cm >5 cm	Very fine Fine Medium Coarse Very coarse	Cracking around burrows and roots Shrinking and swelling in response to drying and wetting
Subangular blocky	Equant to rectangular Dull / rounded interlocking edges	<0.5 cm 0.5–1 cm 1–2 cm 2–5 cm >5 cm	Very fine Fine Medium Coarse Very coarse	Cracking around burrows and roots Shrinking and swelling in response to drying and wetting More deposition and erosion of material than angular blocky peds
Wedge-shaped	Trapezoidal Wedge-shaped with tapering ped faces Slickensides common	<0.5 cm 0.5–1 cm 1–2 cm 2–5 cm >5 cm	Very fine Fine Medium Coarse Very coarse	Substantial shrinking and swelling in response to drying and wetting
Granular	Spheroidal Slight interlocking edges	<1 mm 1–2 mm 2–5 mm 5–10 mm >10 mm	Very fine Fine Medium Coarse Very coarse	Bioturbation Coatings of clay, sesquioxides and organic matter
Crumb	Spheroidal Rounded No interlocking edges	<1 mm 1–2 mm 2–5 mm	Very fine Fine Medium	Bioturbation Coatings of clay, sesquioxides and organic matter (and fecal pellets)
Platy	Tabular Usually horizontal to original land surface	<1 mm 1–2 mm 2–5 mm 5–10 mm >10 mm	Very thin Thin Medium Thick Very thick	Disruption of bedding or laminations Accretion of cementing material common
Prismatic	Elongate Oblong Flat top Usually vertical to original land surface	<1 cm 1–2 cm 2–5 cm 5–10 cm >10 cm	Very fine Fine Medium Coarse Very coarse	Shrinking and swelling in response to drying and wetting
Columnar	Elongate Oblong Domed top Usually vertical to original land surface	<1 cm 1–2 cm 2–5 cm 5–10 cm >10 cm	Very fine Fine Medium Coarse Very coarse	Shrinking and swelling in response to drying and wetting More swelling and percolation of water than prismatic peds

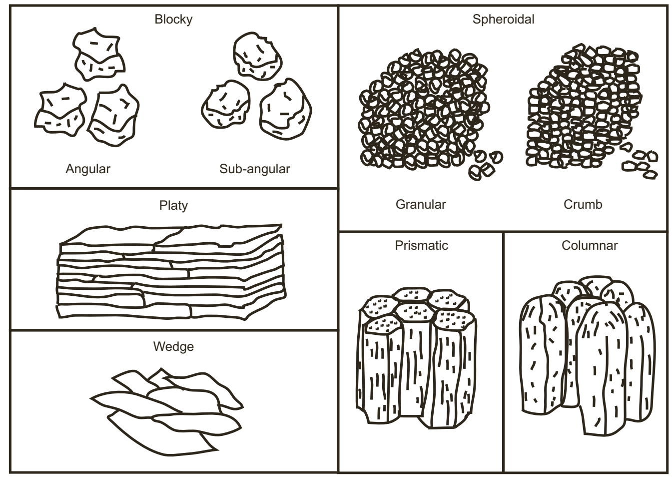

Fig. 6. Schematic diagram of ped shapes, including blocky (angular and sub-angular), spheroidal (granular and crumb), columnar, prismatic, platy and wedge-shaped.

However, in a paleosol the size of peds may fluctuate down-profile, as evidence of repeated sedimentation events coincident with soil formation, especially in composite and compound profiles.

3.3. Pedogenic features

Several features can be observed at the macromorphological scale that reflect pedogenic processes, with general descriptions used to support quantitative methods of paleoclimate reconstruction (Tabor and Myers, 2015). Argillans, mottles, and redoximorphic and vertic features are of particular importance.

Argillans are clayey textural pedofeatures found in soils that experienced sufficient effective precipitation for the downward translocation of clays (Brooks et al., 2012). The type, size, profile depth, abundance, color, and orientation of argillans (or 'clay cutans') should be described. Mack et al. (1993) outlines the primary types of argillans found in paleosols, which include ped, plane, vugh and grain morphologies. Ped argillans are clay coatings or skins that form on peds, whereas plane and vugh argillans are oriented clays that coat planar surfaces and void spaces, respectively (Mack et al., 1993). Grain argillans may be either clay-coated detrital grains (free-grain argillans) or embedded-grain argillans that represent the increase and accumulation of clay down-profile (Mack et al., 1993). Free-grain argillans are also referred to as 'relict cutans' in some aeolian settings (e.g., Fitzsimmons et al., 2009). Argillans should be visually differentiated from the paleosol matrix by their color (Fig. 8A-B), which can also provide clues to the drainage state or hydrological conditions of the soil (Table 8; Tabor and Myers, 2015).

Mottles are secondary soil colors that are different from the matrix color, and typically appear as blotches, spots or streaks. Soil mottling can be the result of biological mixing, mechanical mixing, or the inclusion of weathered substrates (CSIRO, 2009). However, it is commonly associated with variable saturation conditions that create areas of reduction (grey-green) and oxidation (reddish), which are considered redoximorphic features (Vepraskas, 2004). The abundance of mottles is related to the intensity and extent of these redoximorphic conditions, with substantial reduction capable of producing a depleted matrix (gleyed) rather than small patches of color development. The color, abundance and boundary sharpness of mottles should be documented for each horizon (Table 9) along with the type of mottle (e.g., redoximorphic feature, biological mixing). A good rule of thumb is to estimate the abundance across a 0.5 m lateral extent for each horizon, although this will depend on the width of a profile available for description. The morphologies of burrow and rhizolith (rhizohaloes) mottling are more directly related to climatic and environmental conditions and are

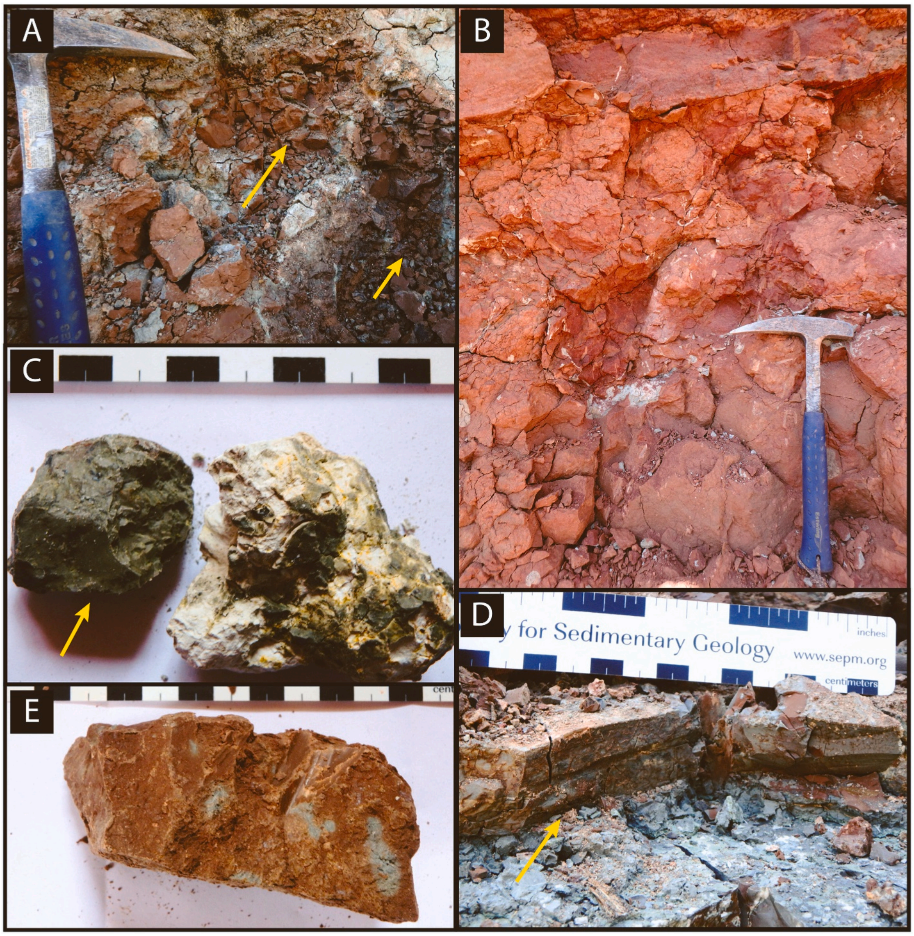

Fig. 7. Examples of common ped shapes in paleosols: A) angular blocky; B) sub-angular blocky; C) granular ped (on left); D) platy; E) angular blocky to wedge-shaped. Scale in A and B is a rock hammer 33 cm long.

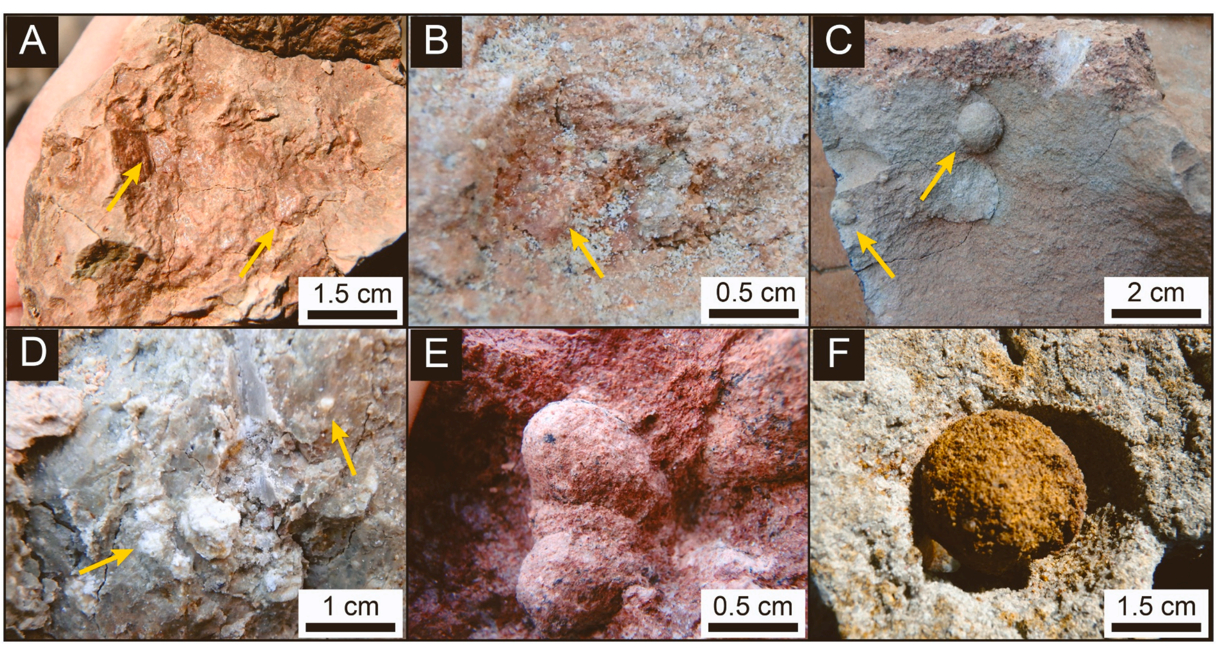

Fig. 8. Examples of common pedogenic features and mineral accumulations in paleosols: A–B) clay plane and ped argillans; C) clay and calcium carbonate nodule; D) filamentous to nodular calcium carbonate accumulations; E) stage II carbonate nodules; F) siderite nodule.

Table 8
Argillan morphologies and their environmental associations. Data sourced from McCarthy et al. (1998) and Tabor and Myers (2015).

Morphology and Color	Paleoenvironmental association
Dark red argillan	Well-drained conditions
Gleyed argillan (low-chroma color)	Periodic to complete saturation
Orange ferri-argillans alternating with black sesquioxide coatings	Alternating Eh-pH conditions; Fluctuating hydrological conditions
Silty clay coatings	Periodic saturation
Yellow clay coatings	Periodic saturation

Table 9
Field description criteria for mottles. Data sourced from CSIRO (2009).

Form	Morphology	Designator
Abundance	0% No mottles or other color patterns	0
	<2% Very few mottles / other color patterns	1
	2–10% Few mottles or other color patterns	2
	10–20% Common mottles or other color patterns	3
	20–50% Many mottles or other color patterns	4
Boundary	Knife-edge boundary between colors	Sharp
	Color transitions in <2 mm	Clear
	Color transitions over >2 mm	Diffuse
Contrast	Indistinct, evident only on close examination	Faint
	Readily evident, but not striking	Distinct
	Striking and conspicuous	Prominent
Size	<5 mm	Fine
	5–15 mm	Medium
	15–30 mm	Coarse
	>30 mm	Very Coarse

outlined in sections 3.5 and 3.6. Both are elongate mottles that form along burrow and root pathways.

Redoximorphic features are the direct result of alternating periods of reductive and oxidative conditions, from the repeated saturation and drying of a profile (Vepraskas, 2004). Redoximorphic features include a reduced matrix, redox concentrations, and redox depletions (Fig. 9). In general, the abundance and strength of redox depletions increases with the duration and intensity of redoximorphic conditions (Vepraskas, 2004). The presence of reduced iron-bearing minerals (principally pyrite and siderite) in a profile is also associated with redoximorphic conditions (Tabor et al., 2017). Table 10 outlines the categories and characteristic morphology of each redoximorphic feature. The type, size, depth in profile, color, orientation, and abundance of each feature should be recorded. For mottling caused by redox concentrations and/or depletions, the general description method for mottles (Table 9) should be followed.

Vertic features are an indication of the shrinking and swelling of clays in response to repeated drying and wetting, and where multiple morphology types are present can be diagnostic of a Vertisol classification (Mack et al., 1993). Five vertic morphologies can be described,

Table 10
Redoximorphic features and their distinguishing morphologies. Data sourced from United States Natural Resources Conservation (2014).

Redoximorphic feature	Category	Morphology
Redox concentrations	Nodules of Fe-Mn oxides	Irregularly shaped Uniform internal structure
	Concretions of Fe-Mn oxides	Irregularly shaped Concentric layers internally
	Masses of Fe-Mn oxides	Mottles of variable shape Reddish in color
	Pore linings of Fe-Mn oxides	Pore surface coatings Impregnations of adjacent matrix
Redox depletions	Fe and Mn depletions	Low chroma mottles Green, grey color mottling Clay content similar to surrounding matrix
	Clay depletions	Low chroma areas with less Fe, Mn and clay than surrounding matrix Common on ped surfaces or lining channels
Reduced matrix	Low chroma matrix	Low chroma soil color Green, grey colors

including desiccation cracks, clastic dikes, hummock and swale structures, slickensides and wedge-shaped peds (Figs. 3B, 7E, 10). The width and depth of desiccation cracks and clastic dikes should be measured, in addition to the sedimentological characteristics of the clastic dike infill. The general dimensions (length, width, height) of slickensides and peds should also be documented. Recording the vertical length of several clastic dikes in a profile can be used as a proxy for burial compaction of a paleosol (Caudill et al., 1997). The length of the dike is determined via the following two methods: i) dividing the dike into several short, straight-line segments, with the length of each segment measured separately and then summed together and ii) measuring the vertical length of the clastic dike along a single straight line (Caudill et al., 1997). Burial compaction is then determined by the following equation:

$$\%\text{compaction} = (\text{vertical length of dike}/\Sigma\ \text{straight line segments})\ \text{x}\ 100$$

Each dike should be measured at least three times with burial compaction determined from the average length, and ideally the overall compaction of the paleosol derived from the average value of at least three discrete clastic dikes if present (Caudill et al., 1997). The presence of desiccation cracks or clastic dikes is also an indication of an A-horizon in Vertisols (e.g. Marriott and Wright, 1993).

Pedogenic slickensides are polished, striated pressure surfaces produced by the frictional movement of one aggregate of soil against another (United States Natural Resources Conservation, 2014). These surfaces form when the shrinking/swelling of clays in response to drying/wetting results in shear failure of the soil (Gray and Nickelsen, 1989). This soil movement also creates wedge-shaped peds at the

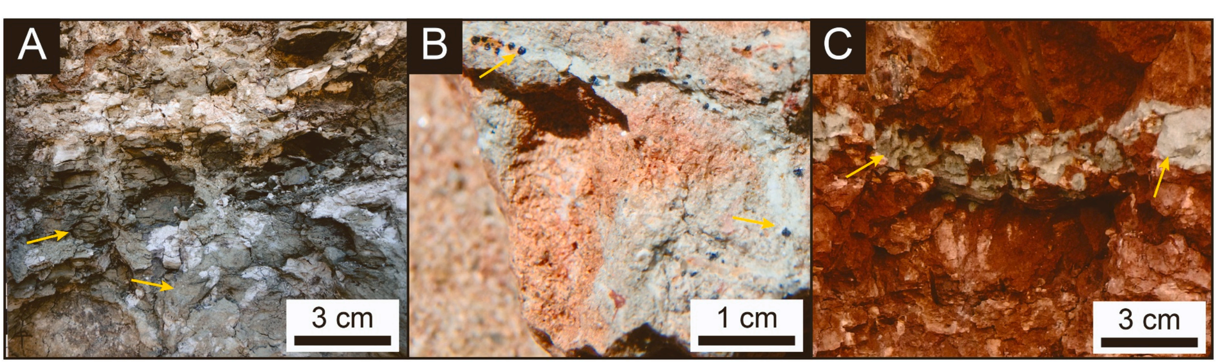

Fig. 9. Examples of redoximorphic features (yellow arrows). A) reduced matrix; B) Pore linings and nodules of Fe-Mn oxides (redox concentrations); C) low chroma areas from Fe and Mn redox depletion. (For interpretation of the references to color in this figure legend, the reader is referred to the web version of this article.)

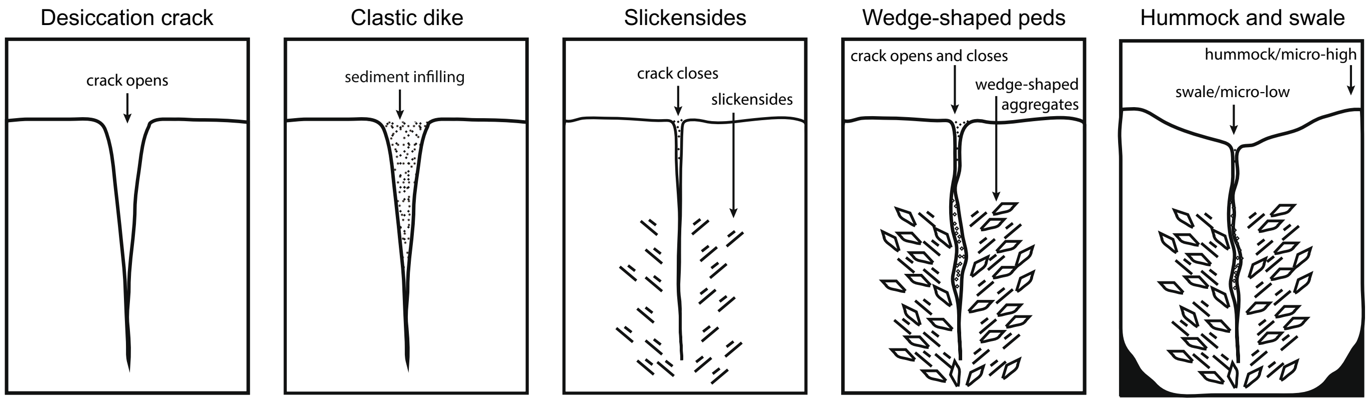

Fig. 10. Schematic diagram of vertic features that form in paleosols, including desiccation cracks, clastic dikes, slickensides, wedge-shaped peds and hummock and swale structure. Vertic morphologies develop over time in response to the shrinking and swelling of clays with repeated wetting and drying. The presence of one or more vertic features, in addition to homogenization of the profile by pedoturbation, is diagnostic of a Vertisol (Mack et al., 1993).

intersection of the shear planes (slickensides) (United States Natural Resources Conservation, 1999). These features can form in soils that comprise expansive clay minerals but are more characteristic of Vertisols (Gray and Nickelsen, 1989; Mack et al., 1993). Slickensides are also described as stress cutans in the Australian Soil Classification (CSIRO, 2009).

3.4. Mineral accumulations

Mineral accumulations are one of the most frequently used features for paleoclimate and paleoenvironment reconstruction of paleosols (e.g., Khademi and Mermut, 1999; Ufnar et al., 2004; Retallack and Huang, 2010; Myers et al., 2012; Orr et al., 2023). Accumulations of carbonates, gypsum, other soluble evaporative-salts, and Fe-Mn oxides are the most described and sampled (Fig. 8C-E). Gypsum and other evaporative-salt (e.g., halite) accumulations are considered evidence of aridity, while carbonate accumulations are an indication of either long-term arid conditions or seasonal aridity (Aslan and Autin, 1998). Fe-Mn oxides are typically associated with redoximorphic conditions (section 3.3). Typically, the type, size (diameter and/or length and width), orientation (presence/absence and direction), and abundance of mineral accumulations are recorded. Carbonate and soluble evaporative-salts (excl. gypsum) form in morphogenetic sequences (Gile et al., 1966; Bockheim, 1990), whereas gypsum and Fe-Mn oxides do not (Vepraskas, 2004; Casby-Horton et al., 2015). Table 11 outlines the different morphological stages of these secondary mineral accumulations, except for Fe-Mn oxides (Table 10).

Calcic and gypsic horizons are especially useful for paleoclimate reconstructions. The depth to either a calcic (DTC) or gypsic (DTG) horizon can be used to quantitatively reconstruct a minimum mean annual precipitation (MAP) value in paleosols that exhibit a complete profile (Retallack, 2005; Retallack and Huang, 2010). The thickness of soil containing stage II carbonates can be used to determine the mean annual range in precipitation (MARP), which represents the difference (in millimeters) between the wettest and driest months (Retallack, 2005). To estimate MAP the depth from the top of the paleosol to the commencement of the calcic or gypsic horizon must be recorded in centimeters. For MARP the total thickness of soil that contains the carbonate nodules is recorded, in centimeters. These depth and thickness measurements should be corrected for compaction prior to deriving MAP or MARP values (see Retallack, 2005; Retallack and Huang, 2010). It is also important to note that DTC- and DTG-derived rainfall estimates are problematic and typically erroneously low because the accuracy of the proxy is dependent on the preservation of a complete soil profile, something rarely seen in the stratigraphic record (Tabor and Myers, 2015). As such, these MAP values should be regarded as minimums and should be supported by sedimentological evidence (e.g., presence or absence of salts, mottling or redoximorphic features) (e.g., Prochnow et al., 2006; Mouraviev et al., 2019; Orr et al., 2021).

3.5. Burrows and chambers

Burrows are trace fossils that can record paleo-infaunal diversity and inform paleoenvironmental interpretations (Cleveland et al., 2008). These trace fossils are commonly preserved in paleosols as either actively or passively filled structures (Hembree and Bowen, 2017). Actively filled burrows contain obliquely or vertically laminated sediments and fecal pellets created by the burrower, whereas passively filled burrows typically contain horizontally laminated sediment that is compositionally similar to the overlying unit (Fig. 11A-F) (Knaust and Bromley, 2012). The tunnels can be passively filled by draught filling (e.g., Goldring, 1996; Wetzel et al., 2014) or gravitational collapse (e.g., Loope, 2008; Hembree, 2019), in the case of the latter the sediment will more likely be compositionally similar to the surrounding unit. Burrow morphology parameters are varied (Hembree and Bowen, 2017) and should be recorded, including the color (mottles, rims and matrix), diameter, length, orientation (horizontal, sub-vertical or vertical), tunnel tortuosity (straight or sinuous) and whether the burrow displays a branching or non-branching structure. The burrow fill, including color, internal structure (lined or unlined) and sedimentological characteristics, should also be documented. These morphologies are attributed to a variety of environments and fauna and are particularly useful for ecological interpretations (Table 12).

However, the most common type of insect traces observed in paleosols are chambers (Genise, 2017). These chambers are associated with a large array of insects and for various functions, such as pupation, brooding or nesting (Genise, 2017). Chambered trace fossils may be recognized by their regular shape and size (Fig. 12) and may or may not be preserved with burrows. The distinct shape and markings of a chamber can be used to discern a trace fossil from four potential ichnofamilies: Celliformidae, Krausichnidae, Coprinisphaeridae and Pallichnidae.

Celliforma traces always comprise cells. These cells may be singular, in groups or attached to tunnels, and are formed by bees (Genise, 2000). Krausichnidae are represented by chambers with burrow systems (or boxworks) of different diameters, and are associated with ants and termites (Genise, 2004). Coprinisphaera are perhaps the most recognized insect trace fossil in paleosols. Coprinisphaera traces are mostly formed by ants, bees, beetles, termites, and wasps (Genise et al., 2000), and are preserved as isolated or clustered chambers that lack burrows (Genise, 2017). The chambers may be spherical, ellipsoid, ovate or pear-shaped, and a discrete thick lining should be present (Genise, 2017). Pallichnidae are determined by the presence of an unlined spherical, hamate, ovoid or lunate chamber created by beetles (Genise, 2004, 2017). The

Table 11
Morphology of carbonate, gypsum, and other evaporative-salt accumulations. Data sourced from (Gile et al., 1966; Machette, 1985; Bockheim, 1990; Mack et al., 1993).

Mineral	Stage	Morphology
Carbonate (in paleosols developed in gravel)	I	Filaments and thin discontinuous grain coatings
	II	Nodules (Diffuse and poorly cemented to discrete and well-cemented masses) Continuous coating around and/or between clasts
	III	Massive carbonate beds or continuous indurated horizons
Carbonate (in paleosols developed in sand, silt or clay)	I	Dispersed powdery and filamentous carbonate
	II	Few to common carbonate nodules and veinlets with powdery and filamentous carbonate in between nodules
	III	Nodules coalesce to form a continuous carbonate layer Isolated nodules with powdery carbonate outside main horizon
Carbonate (in paleosols developed in gravel, sand, silt or clay)	IV	Indurated horizons topped by weakly developed laminar deposits
	V	Strongly developed platy or lamellar cap on the carbonate layer Some brecciation with carbonate pisolites of laminar deposit
	VI	Brecciation and recementation Pisoliths common in the upper laminar layer
Gypsum	n/a	Gypsum or anhydrite filled desiccation cracks
	n/a	Displacive and replacive nodular and enterolithic textures of gypsum or anhydrite
	n/a	Multiple erosion surfaces due to capillary draw of gypsum and/or anhydrite precipitation, followed by erosion by wind or water
	n/a	Gypsum or anhydrite associated tepee structures
	n/a	Gypsum or anhydrite associated columnar peds
	n/a	Gypsum or anhydrite ped or grain cutans, or vugh or plane linings
Other evaporative salts	0	No salt
	1	Salt encrustations beneath clasts
	2	Salt flecks covering <20% of the horizon area
	3	Salt flecks covering >20% of the horizon area
	4	Weakly cemented salt pan
	5	Strongly cemented salt pan
	6	Indurated salt pan.

shape and size of insect trace fossils vary extensively, and the reader is referred to Genise (2017) for a comprehensive review of shapes, walls and fillings and their insect group associations.

3.6. Root traces

Root structures represent preservation of evidence of vascular plants (Klappa, 1980a), and may be differentiated from burrows by their general morphological characteristics (Retallack, 1988), which include cylindrical structures (circular in cross-section) that are a few centimeters to several meters in length that may be vertically isolated or branching. Roots that branch will bifurcate downwards with a decreasing diameter between the second, third and fourth order branches, whereas a burrow's diameter remains unchanged.

Root structures are formerly identified as *rhizoliths* and are classified by their morphology and the degree of mineral replacement and/or impregnation (Figs. 11G-L, 13; Table 13) (Klappa, 1980a). The classification scheme is supplemented by vadose texture descriptions, including alveolar (sub-mm, closely spaced root molds), vermicular (spaghetti-like calcified root hairs), and the presence of calcrete rhizobrecciation (angular to subrounded fragments of calcrete in undifferentiated micritic matrix) or tepee structures (rhizobrecciated fragments in pseudo anticlines) (Klappa, 1980b).

Detailed rhizolith morphology is essential for paleoenvironmental interpretations (Table 14). The color of rhizoliths, their rims, and the immediately surrounding matrix are particularly diagnostic of the moisture content and drainage state of a soil (Fig. 13; Kraus and Hasiotis, 2006). Interpretations may also be made regarding the general morphology of root systems. Laterally spreading root systems can be an indication of either waterlogged or indurated lower soil environments, as roots rarely penetrate these horizons (Retallack, 1988). Root systems in Cenozoic and potentially some Cretaceous paleosols that are predominantly fibrous and contain roots smaller than 2 mm in diameter are typically attributed to grasses (Retallack, 1988). These systems are associated with open grassland environments and dry climates where they appear less branched and more clumped (Weaver, 1968), however documentation of such features in pre-Cretaceous paleosols are unrelated to grasses and cannot be linked to these climatic or environmental conditions. Rhizoliths with large diameters typically indicate woody vegetation and greater maximum rooting depths in late Paleozoic-Cenozoic ecosystems (Gocke et al., 2014), however, there are exceptions such as with Carboniferous lycopsid trees where this does not apply (as they did not produce woody roots; e.g., Hetherington and Dolan, 2017) or the early Calamite trees that utilized horizontal rhizomes (e.g., Feng, 2017). Root systems that deeply penetrate a soil may be associated with either a well-drained soil (Sarjeant, 1975), or a soil of low strength (Valentine et al., 2012), which is usually attributed to soil type, with porous soils, such as sandy loams, possessing lower strength (Whalley et al., 1995).

Several additional rhizolith parameters can be measured to enhance paleoecological reconstructions (do Nascimento et al., 2019). These parameters include the number, diameter, length, length density, and the branching angle and pattern of the roots (Table 15). Each variable can be measured within a 0.5 m × 0.5 m area, with data collected independently for large and small rhizoltihs (e.g., Gocke et al., 2014). For paleosols with exposures >0.5 m, three such areas can be recorded, and the average and standard error reported, whereas for smaller exposures (such as core samples) measurements are limited to the exposed area. Comparative analysis with modern root systems is typically required to determine the full significance of the collected data. However, this is only relevant when examining paleosols that are young enough to have hosted similar vegetation types, such as the Cenozoic. For paleosols that developed in the Cretaceous and earlier these measurements can still determine both the typology and geometry of the root system (do Nascimento et al., 2019), and comparisons may be made across the literature. Importantly, collecting such measurements as a standard can enhance our communication of observations and understanding of the paleoecology and paleoenvironment across the geologic time scale.

Comprehensive root length and maximum root depth measurements in a profile may also improve our understanding of the ecological system through paleobiome interpretation (Table 16). However, it is important to note biome-maximum rooting depth associations are currently based on modern observations only and may have limited applicability for the paleorecord. We provide them here as they may prove helpful to those examining Cenozoic paleosols as they formed after the advent of angiosperms in the Mesozoic. However, given the changes in plant architecture through time (Gastaldo and Demko, 2011), these biome-associations are not considered applicable to paleosols that predate the evolution of higher vascular plants in the Late Silurian or seed plant ecosystems in the Late Devonian. Maximum rooting depth measurements should also be treated as minimums; as discussed previously, complete paleosol profiles are rarely preserved and the amount of soil removed prior to preservation is unclear.

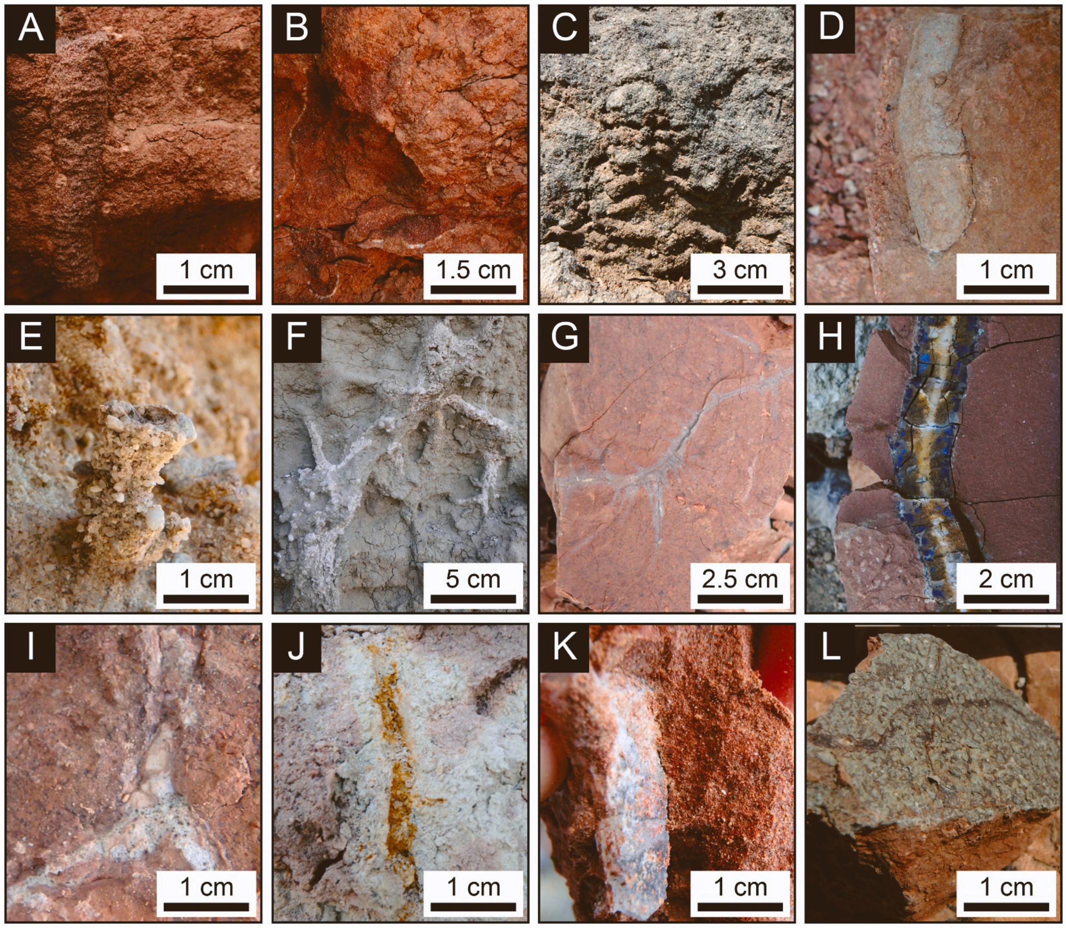

Fig. 11. Examples of burrows and rhizoliths in paleosols. A–C) sediment infilled burrows; D) burrow concretion (calcium carbonate); E) sediment infilled burrow; F) calcium carbonate infilled burrows; G) mottled root trace; H) Rhizocretion with Mn-oxide and calcium carbonate accumulation; I) root cast with calcium carbonate accumulation; J) silica replaced root cast with Fe-oxide accumulation; K) sparite replaced root cast; L) carbonized root trace with Mn- and Mg-oxide staining.

4. Sampling

4.1. Matrix

Bulk matrix samples should be collected from each horizon, and it is recommended that standardized data collection methods be used and recorded. A template to assist with standardization of sample collection data has been developed to assist with sampling (Appendix B). The amount of material that is required will depend on the analyses to be completed in the future, with more material required for a larger array of analyses. Bulk samples are often used for determining major, trace and rare earth elemental compositions (REE), mineralogy, and the stable carbon-isotope composition of organic matter. Samples from each horizon can also be used to prepare thin sections and determine down profile changes at the micromorphological scale. Therefore, we recommend at least two ~10 cm cube samples from each horizon, with one coherent enough for thin section preparation (e.g., Retallack, 1997), to ensure enough sample material. Where horizons are particularly thick, such as B-horizons in cumulate profiles, and intra-horizon variation is of interest, more samples can be collected (e.g., at 10 cm intervals). Most samples do not require special handling and may be collected using a standard geological hammer and sample bags; however, if *n*-alkanes are being considered it is particularly important to recall that samples must not come in contact with plastic sampling equipment or bags.

Quantitative paleoclimate reconstruction is usually achieved through major element analysis via X-ray fluorescence spectrometry (XRF) and mineralogical analysis via X-ray diffraction (XRD) (Sheldon and Tabor, 2009; Tabor and Myers, 2015). A minimum of 10 g each for XRF and XRD is typically required by most laboratories, although 20–30 g is preferred (e.g., Mineral Technologies, ALS Global) (A, Locke, per comms, Nov 2019). Trace element and REE may be determined using Laser Ablation Inductively Coupled Plasma Mass Spectrometry (LA-ICP-MS), requiring an additional few grams of sample, although many laboratories can use the residual sample following XRF analysis (Y. Hu, per comms, April 2019). Stable carbon isotope analyses of organic matter conducted on an elemental analyzer coupled to an isotope ratio mass spectrometer (EA-IRMS) usually only requires a few milligrams (J. Whan, per comms, Jan 2020).

Paleovegetation studies that examine pollen, phytoliths or *n*-alkanes, can require additional sample material. In particular *n*-alkanes, where up to 100 g may be needed (R. Comley, per comms, Feb 2021). Samples for pollen and phytoliths do not require any special handling other than minimizing potential surface contamination with modern sediments. However, material for *n*-alkanes should only be sampled and stored using metal or glass utensils (Brocks et al., 2008). Contact with any plastic material will contaminate and compromise the sample by overprinting the biomarker profile (Brocks et al., 2008).

4.2. Mineral accumulations

Secondary mineral accumulations are frequently used for paleoclimate and paleoenvironment reconstruction of paleosols (e.g., Driese et al., 1992; Nordt et al., 2006; Cerling et al., 2011; Myers et al., 2012; Orr et al., 2021). In particular, carbonates, gypsum, goethite and siderite

Table 12
Examples of burrow morphologies and their environment and faunal associations. Data sourced from Hembree and Bowen and references therein (2017).

Burrow morphology	Environment association	Faunal attribution
Green mottled channels	Abundant organic material Moderately well-drained Moist	Surface-active detritivores Soil-dwelling deposit feeders
Red-rims	Oxidation of matrix prior to filling	None
Meniscate filled	Moderately to well-drained Soil moisture 5–45%	Larval insects
O- and J- shaped	Decomposing vegetation Seasonal climate	Millipedes
Simple meandering, meniscate filled burrows with sharp walls)	Low organic content Moderately well-drained Moist	Soil-dwelling deposit feeders (e.g., larval insects, symphyla and some mites)
Heterogeneous passively filled	Moderately to well-drained	Adult and larval insects Millipedes Small vertebrates
Lined homogenous passively filled	Various	Small predatory arthropods (e.g., scorpions and spiders)
Unlined, J- shaped homogenous passively filled	Moderately to poorly drained	Millipedes
Sinuous, spar-filled	Seasonal climate Moderately to well-drained	Larval insects

accumulations can provide valuable quantitative data (Tabor and Myers, 2015). It is helpful to place mineral accumulation samples into separate bags from the bulk matrix to make subsequent sample identification and laboratory work easier.

Calcium carbonate accumulations can be sampled for stable-isotope analyses. The isotopic composition of calcium carbonates can be used for vegetation ratio determinations (C_3/C_4 photosynthesizing plants) (Wang and Zheng, 1989), atmospheric CO_2 concentrations (Cerling, 1992), paleoelevation (Ghosh et al., 2006), and mean annual temperature (Dworkin et al., 2005). Calcium carbonate accumulations should only be sampled if they represent Stage II pedogenic nodules, are from a fresh surface and at depths >30 cm (preferably >50 cm) to limit the effects of diffusional mixing with atmospheric CO_2 (Cerling et al., 1989; Cerling et al., 1991; Cerling and Quade, 1993). The sampling depth of the nodules should be recorded and can be examined in the context of the Cerling et al. (1991) soil CO_2 diffusion-reaction model. A minimum of three nodules per profile should be sampled to provide an average isotopic composition and account for internodular variability (e.g., Nordt et al., 2003; Huang et al., 2012); although a higher number is recommended to obtain a more representative sample. Individual nodules can also be sampled and analyzed multiple times to capture intra-nodule variability. Nodules as small as 4 mm in diameter may be collected (e.g., Rochín-Bañaga et al., 2024), but should not exceed ~10 mm (~pea-sized) as larger accumulations may contain multiple phases of carbonate growth. A narrow distribution in isotopic values would suggest the pedogenic carbonate had not been overprinted or recrystallized and formed in a stable precipitational environment (Deutz et al., 2001; Defliese and Lohmann, 2015). Micromorphological analysis of the carbonates to confirm the presence of unaltered micritic material is also required. Rhizoliths with calcium carbonate accumulation can be selected for subsequent U/Pb dating. It is imperative that first generation micritic samples be used to ensure an accurate geochronological analysis (Wang et al., 1998). Sparry textures indicate recrystallization or secondary precipitation and should be avoided.

Goethite nodules, or ferrans, can be sampled for stable oxygen- and carbon- isotope compositional analysis and used to estimate atmospheric CO_2 concentrations (Tabor et al., 2004). Accumulations are mostly found in the upper horizons, can be nodular or vermiform, and are usually light to dark brown (e.g., Löhr et al., 2013). Examples from the available literature suggest collecting samples from >40 cm down profile (e.g., Tabor et al., 2004). Individual nodules can be hand-picked,

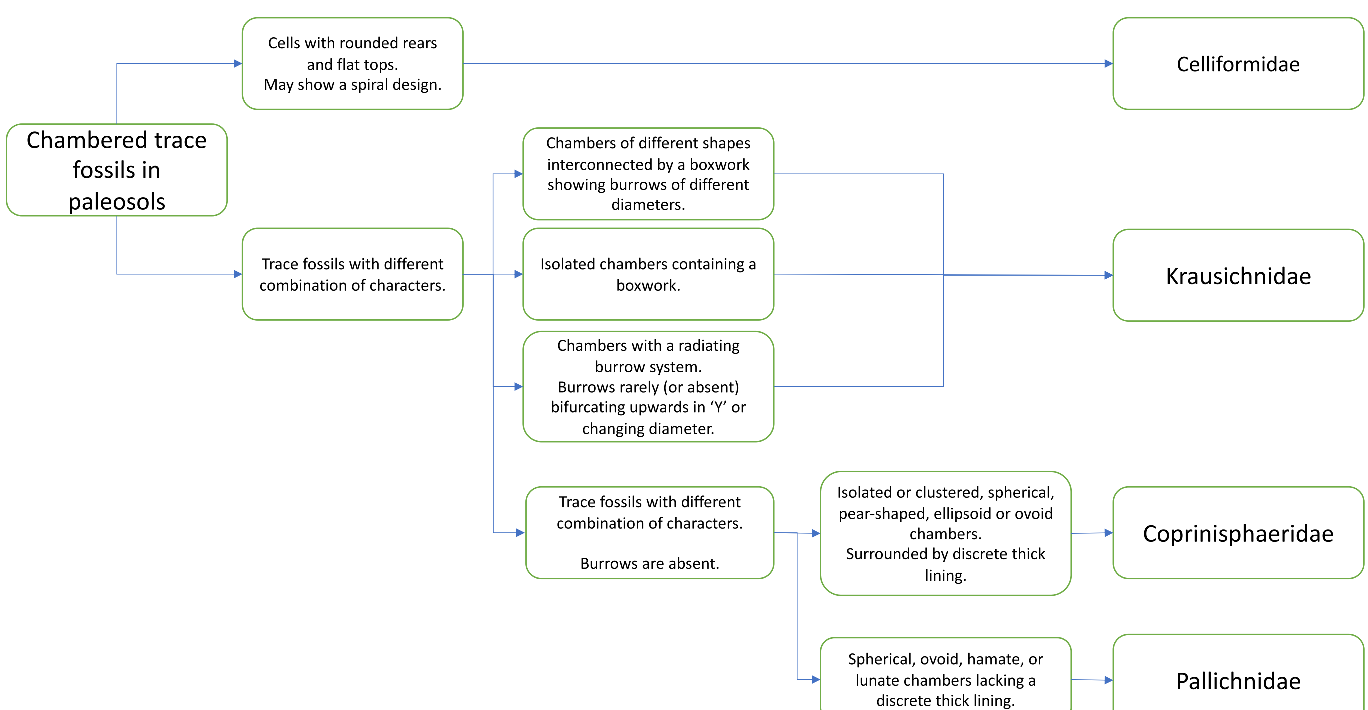

Fig. 12. Distinguishing morphologies of select chambered trace fossils in paleosols. Data sourced from (Genise, 2017). The reader is directed to Genise (2017) for illustrations of each ichnofamily and further diagnostic properties to interpret insect associations.

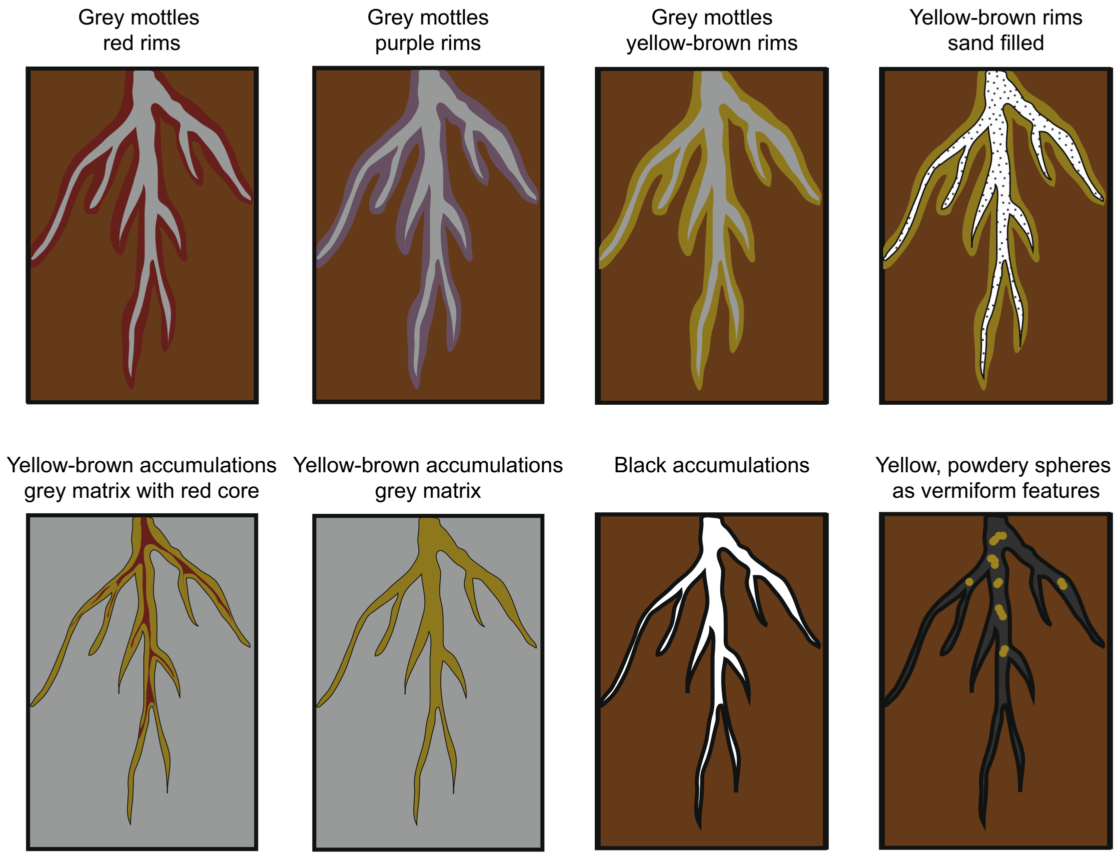

Fig. 13. Schematic diagram of rhizolith morphologies that form in response to varying drainage conditions. Rims of red and purple generally indicate moderately well-drained conditions, yellowish rims and/or accumulations form in poorly drained environments and black accumulations (e.g., Mn-oxide spherules) in very poorly drained conditions. Grey mottled channels represent zones of depletion. (For interpretation of the references to color in this figure legend, the reader is referred to the web version of this article.)

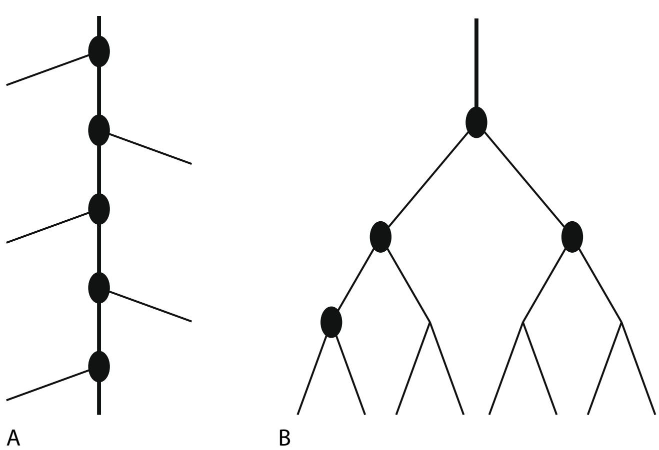

Fig. 14. Generalized schematics of herringbone (A) and dichotomous (B) root structures. Modified after Xiaoting et al. (2019).

Table 13
Rhizolith classification according to genesis and morphology. Data sourced from Klappa (1980a) and Kraus and Hasiotis (2006).

Rhizolith	Morphology
Rhizohalo	Mineral depletions around a root (distinguished by color variation from matrix)
Root molds	Tubular voids
Root casts	Sediment and/or cement filled root molds
Root tubules	Cemented cylinders around root molds
Rhizocretions	Pedodiagenetic mineral accumulations around root structures (living or dead)
Root petrifaction	Mineral impregnation or replacement of organic matter Partial or total preservation of root anatomical features

or separated from the matrix by sieving if the profile is unlithified. The iron oxide-hydroxide is not as commonly used as pedogenic carbonate for $p\mathrm{CO_2}$ reconstructions but is a valuable option with smaller uncertainties (Tabor and Myers, 2015).

The δ^{18}O and δ^{13}C values of pedogenic siderite and sphaerosiderite are used in paleoclimatic analyses to construct meteoric sphaerosiderite lines, assess methane oxidation (Ufnar et al., 2001), and investigate changes in the hydrologic cycle (Ludvigson et al., 2013). These mineral accumulations often form sub-mm nodules that are yellowish brown to black (siderite; Fig. 8F) or greyish to reddish brown (sphaerosiderite) (e.g., Ludvigson et al., 2013). However, pedogenic siderite and sphaerosiderite accumulations are often on a microscopic scale and may be overlooked in a profile; however, their association with wetland settings can help the sampler identify likely host paleosols (Ludvigson et al., 2013). Reports in the literature suggest a minimum of 10 siderite or sphaerosiderite accumulations should be sampled (Ufnar et al., 2001). However, sufficient material must be sampled for i) microsampling by milling for isotopic analysis (Ludvigson et al., 2013) and ii) preparation of thin sections for confirmation of unaltered, early diagenetic material (Ufnar et al., 2001). In many cases it may only be possible to collect matrix samples and extract microcrystalline siderite accumulations gravimetrically in the laboratory (e.g., Driese et al., 2010).

Gypsum accumulations also can be sampled where there is an interest in reconstructing paleohydrology. The δD and δ^{18}O values of

Table 14
Examples of rhizolith morphology and their associated paleoenvironments and geochemical profiles. Data sourced from Kraus and Hasiotis (2006).

Rhizolith morphology	Rhizolith	Environmental and geochemical associations
Calcareous accumulations	Rhizocretions	Moderately well-drained soils Episodic drying for long periods
Grey mottles with red rims	Rhizohaloes	Moderately well-drained soils Fe depletion and hematite accumulation Moderate surface-water gley processes
Grey mottles with purple rims	Rhizohaloes	Moderately well-drained soils Fe depletion and hematite accumulation Extensive surface-water gley processes
Grey mottles with yellow-brown rims	Rhizohaloes Rhizotubules	Poorly drained soils Fe depletion and goethite accumulation Surface-water gley processes High moisture content and organic matter
Yellow-brown accumulations, in grey matrix	Rhizocretions	Poorly drained soils Fe depletion and goethite accumulation Lignite accumulation (organic matter preservation) Sustained reducing conditions e.g., marsh
Yellow-brown tendrils, in grey matrix, often with red core	Rhizocretion	Poorly drained soils Fine roots Goethite and hematite accumulation Wet and anoxic environment, Wetland plants with aerenchyma
Yellow, powdery spheres as vermiform features	Rhizocretions	Poorly drained soils Jarosite, native sulfur, pyrite, and gypsum accumulations Organic rich soils Sustained periods of reducing conditions
Yellow-brown rims, sand filled	Rhizotubules	Goethite accumulation Preservation of subterranean root systems
Black accumulations	Rhizotubules	Poorly drained soils Mn-oxide and goethite accumulation Organic matter fossil preservation Typically silt-rich or clay-rich soils Alternating reducing and oxidizing conditions
Carbonaceous strands in rhizolith with yellow accumulations	All Forms	Very poorly drained soils Fe and Mn-oxide accumulations Jarosite accumulation Organic matter fossils
Concentrations of small black spheres in grey matrix	Rhizotubules	Very poorly drained soils Fe- and Mn-oxide accumulation

gypsum crystallization water can be used to establish meteoric water lines (Khademi et al., 1997), while the triple oxygen and hydrogen isotopes of gypsum-hydration water can quantitatively reconstruct paleo-humidity (Gázquez et al., 2018). Individual gypsum crystals or accumulations may be hand-picked from bulk matrix samples (Khademi et al., 1997).

5. Conclusion

Paleosols form in response to climatic and environmental conditions, and their retention of biological, chemical, and physical information provides an unequalled resource of terrestrial climate records. Where paleosols form in rift, strike-slip or other such basins, with high sediment accumulation rates, these records are often of high-resolution. The geographical and temporal ubiquity of paleosols suggests these terrestrial records deserve greater attention. Not only can paleosols enhance the continental climate record throughout geologic time but can bridge the gap between paleontology and sedimentology, by providing detailed environmental information. This guide builds upon previous works by others that focused on field recognition and classification of paleosols, by providing detailed logging procedures and sampling instructions, with a particular focus on which measurements should be recorded for various pedogenic features. The provision of minimum sample weights required for different mineralogical and geochemical analyses, and the step-by-step field-testing guide with standardized logging and sample collection templates, should prove useful. It is also intended that the description of observations needed from burrow and root structures for accurate paleoecological reconstruction prove useful. Above all, this guide was created to help any earth scientist enter the field armed with the information needed to competently recognize, classify, document, and test paleosols, while collecting appropriate samples of sufficient amounts for subsequent laboratory analyses, and the generation of viable and publishable data.

Table 15
Measurable rhizolith parameters and their paleoecological associations. Data from Gocke et al. (2014), and do Nascimento et al. (2019), modified after Atkinson (2000).

Rhizolith parameter	Required measurement	Paleoecological association
Number	Total number of individual roots	Presence of roots in volume of soil
Diameter	Diameter of roots (mm)	Rooting depth indicator Vegetation functional group
Length	Length of roots (mm)	Root system size Soil strength (penetrative resistance)
Length density	Length of roots per unit of soil volume	Soil nutrient and water availability
Branching angle	Angle between branches	Absorption and nutrient interception
Branching pattern	Herringbone – Dichotomous *Refer to* Fig. 14	Intensity of soil exploitation

Table 16
Maximum rooting depth and biome associations. Data sourced from Canadell et al. (1996).

Maximum rooting depth	Modern biome association
2.0 ± 0.3 m	Boreal forest
9.5 ± 2.4 m	Desert
5.2 ± 0.8 m	Sclerophyll shrubland and forest
3.9 ± 0.4 m	Temperate coniferous forest
2.9 ± 0.2 m	Temperate deciduous forest
2.6 ± 0.2 m	Temperate grassland
3.7 ± 0.5 m	Tropical deciduous forest
7.3 ± 2.8 m	Tropical evergreen forest
15.0 ± 5.4 m	Tropical grassland/savanna
0.5 ± 0.1 m	Tundra

Declaration of competing interest

The authors declare that they have no known competing financial interests or personal relationships that could have appeared to influence the work reported in this paper.

Data availability

No data was used for the research described in the article.

Acknowledgements

This work was supported by PhD scholarship and research funding from James Cook University to T. Orr. Additional fieldwork expenses were supported by the U.S. National Science Foundation grants (EAR-0617561, BCS-1638796 and EAR-1349825). We would like to thank S. Askew, R. Comley, B. Jones, J. Whan, and C. Wurster for their guidance on laboratory protocols. Special thanks to N.J. Stevens, P.M. O'Connor, L. Lawrence and C. Mtelela for field assistance. We also thank K. Behrensmeyer and A. Racey for reviewing an early draft of this manuscript, and the editor (C. Fielding), N. Tabor, M.S. Raigemborn and two anonymous reviewers for their constructive feedback, which greatly improved the manuscript.

Appendix A. Supplementary data

Supplementary data to this article can be found online at https://doi.org/10.1016/j.earscirev.2024.104788.

References

Aslan, A., Autin, W.J., 1998. Holocene flood-plain soil formation in the southern lower Mississippi Valley: implications for interpreting alluvial paleosols. GSA Bull. 110 (4), 433–449.

Atkinson, D., 2000. Root characteristics: Why and what to measure. In: Root methods. Springer, pp. 1–32.

Babechuk, M.G., Kamber, B.S., 2013. The Flin Flon paleosol revisted. Can. J. Earth Sci. 50, 1223–1243.

Beverly, E.J., Peppe, D.J., Driese, S.G., Blegen, N., Faith, J.T., Tryon, C.A., Stinchcomb, G.E., 2017. Reconstruction of late Pleistocene paleoenvironments using bulk geochemistry of paleosols from the Lake Victoria region. Front. Earth Sci. 5, 93.

Birkeland, P.W., 1999. Soils and Geomorphology, 3rd ed. Oxford University Press.

Bockheim, J., 1990. Soil development rates in the Transantarctic Mountains. Geoderma 47 (1–2), 59–77.

Brocks, J.J., Grosjean, E., Logan, G.A., 2008. Assessing biomarker syngeneity using branched alkanes with quaternary carbon (BAQCs) and other plastic contaminants. Geochim. Cosmochim. Acta 72 (3), 871–888.

Brooks, E.S., Boll, J., McDaniel, P.A., 2012. Chapter 10 – Hydropedology in seasonally dry landscapes: The Palouse Region of the Pacific Northwest USA. In: Lin, H. (Ed.), Hydropedology. Academic Press, pp. 329–350.

Broz, A.P., 2020. Organic matter preservation in ancient soils of Earth and Mars. Life 10, 113.

Canadell, J., Jackson, R., Ehleringer, J., Mooney, H., Sala, O., Schulze, E.D., 1996. Maximum rooting depth of vegetation types at the global scale. Oecologia 108, 583–595.

Casby-Horton, S., Herrero, J., Rolong, N.A., 2015. Chapter four – Gypsum soils—their morphology, classification, function, and landscapes. In: Sparks, D.L. (Ed.), Advances in Agronomy, vol. 130. Academic Press, pp. 231–290.

Caudill, M.R., Driese, S.G., Mora, C.I., 1997. Physical compaction of vertic palaeosols: implications for burial diagenesis and palaeo-precipitation estimates. Sedimentology 44 (4), 673–685.

Cerling, T.E., 1992. Use of carbon isotopes in paleosols as an indicator of the P(CO2) of the paleoatmosphere. Glob. Biogeochem. Cycles 6 (3), 307–314.

Cerling, T.E., Quade, J., 1993. Stable carbon and oxygen isotopes in soil carbonates. Climate change in continental isotopic records, pp. 217–231.

Cerling, T.E., Quade, J., Wang, Y., Bowman, J., 1989. Carbon isotopes in soils and palaeosols as ecology and palaeoecology indicators. Nature 341 (6238), 138–139.

Cerling, T.E., Solomon, D.K., Quade, J., Bowman, J.R., 1991. On the isotopic composition of carbon in soil carbon dioxide. Geochim. Cosmochim. Acta 55 (11), 3403–3405.

Cerling, T.E., Wynn, J.G., Andanje, S.A., Bird, M.I., Korir, D.K., Levin, N.E., Mace, W., Macharia, A.N., Quade, J., Remien, C.H., 2011. Woody cover and hominin environments in the past 6 million years [Article]. Nature 476, 51.

Cleveland, D.M., Nordt, L.C., Atchley, S.C., 2008. Paleosols, trace fossils, and precipitation estimates of the uppermost Triassic strata in northern New Mexico. Palaeogeogr. Palaeoclimatol. Palaeoecol. 257 (4), 421–444.

CSIRO, 2009. Australian Soil and Land Survey Field Handbook, 3rd ed. CSIRO Publishing.

Defliese, W.F., Lohmann, K.C., 2015. Non-linear mixing effects on mass-47 clumped isotope thermometry: patterns and implications. Rapid Commun. Mass Spectrom. 29, 901–909.

Demko, T.M., Currie, B.S., Nicoll, K.A., 2004. Regional paleoclimatic and stratigraphic implications of paleosols and fluvial/overbank architecture in the Morrison formation (Upper Jurassic), Western Interior, USA. Sediment. Geol. 167, 115–135.

Deutz, P., Montañez, I.P., Monger, H.C., Morrison, J., 2001. Morphology and isotope heterogeneity of Late Quaternary pedogenic carbonates: Implications for paleosol carbonates as paleoenvironmental proxies. Palaeogeogr. Palaeoclimatol. Palaeoecol. 166, 293–317.

Do Nascimento, D.L., Batezelli, A., Ladeira, F.S.B., 2019. The paleoecological and paleoenvironmental importance of root traces: plant distribution and topographic significance of root patterns in Upper Cretaceous paleosols. Catena 172, 789–806.

Driese, S.G., Mora, C.I., Cotter, E., Foreman, J.L., 1992. Paleopedology and stable isotope chemistry of Late Silurian vertic Paleosols, Bloomsburg Formation, Central Pennsylvania. J. Sediment. Res. 62 (5).

Driese, S.G., Mora, C.I., Stiles, C.A., Joeckel, R.M., Nordt, L.C., 2000. Mass-balance reconstruction of a modern Vertisol: implications for interpreting the geochemistry and burial alteration of paleo-Vertisols. Geoderma 95 (3), 179–204.

Driese, S.G., Ludvigson, G.A., Roberts, J.A., Fowle, D.A., González, L.A., Smith, J.J., Vulava, V.M., McKAy, L.D., 2010. Micromorphology and stable-isotope geochemistry of historical pedogenic siderite formed in Pah contaminated alluvial clay soils, Tennessee, U.S.a. J. Sediment. Res. 80, 943–954.

Dworkin, S., Nordt, L., Atchley, S., 2005. Determining terrestrial paleotemperatures using the oxygen isotopic composition of pedogenic carbonate. Earth Planet. Sci. Lett. 237 (1), 56–68.

Feng, Z., 2017. Late Palaeozoic plants. Curr. Biol. 27(17, R905–R909.

Fitzsimmons, K.E., Magee, J.W., Amos, K.J., 2009. Characterisation of aeolian sediments from the Strzelecki and Tirari Deserts, Australia: implications for reconstructing palaeolenvironmental conditions. Sediment. Geol. 218 (1–4), 61–73.

Gastaldo, R.A., Demko, T.M., 2011. The relationship between continental landscape evolution and the plant-fossil record: Long term hydrologic controls on preservation. In: Taphonomy: Process and bias through Time. Springer, pp. 249–285.

Gázquez, F., Morellón, M., Bauska, T., Herwartz, D., Surma, J., Moreno, A., Staubwasser, M., Valero-Garcés, B., Delgado-Huertas, A., Hodell, D.A., 2018. Triple oxygen and hydrogen isotopes of gypsum hydration water for quantitative paleo-humidity reconstruction. Earth Planet. Sci. Lett. 481, 177–188.

Genise, J.F., 2000. The ichnofamily Celliformidae for Celliforma and allied ichnogenera. Ichnos Int. J. Plant Anim. 7 (4), 267–282.

Genise, J.F., 2004. Ichnotaxonomy and ichnostratigraphy of chambered trace fossils in palaeosols attributed to coleopterans, ants and termites. Geol. Soc. Lond. Spec. Publ. 228 (1), 419–453.

Genise, J.F., 2017. Ichnoentomology: Insect Traces in Soils and Paleosols. Springer.

Genise, J.F., Mangano, M.G., Buatois, L.A., Laza, J.H., Verde, M., 2000. Insect trace fossil associations in paleosols: the Coprinisphaera ichnofacies. Palaios 15 (1), 49–64.

Ghosh, P., Garzione, C.N., Eiler, J.M., 2006. Rapid uplift of the Altiplano revealed through 13C-18O bonds in paleosol carbonates. Science 311 (5760), 511–515.

Gile, L.H., Peterson, F.F., Grossman, R.B., 1966. Morphological and genetic sequences of carbonate accumulation in desert soils. Soil Sci. 101 (5), 347–360.

Gocke, M., Gulyás, S., Hambach, U., Jovanović, M., Kovács, S.B., Marković, B., Wiesenberg, G.L.B., 2014. Biopores and root features as new tools for improving paleoecological understanding of terrestrial sediment-paleosol sequences. Palaeogeogr. Palaeoclimatol. Palaeoecol. 394, 42–58.

Goldich, S.S., 1984. Determination of ferrous iron in silicate rocks. Chem. Geol. 42 (1–4), 343–347.

Goldring, R., 1996. The sedimentological significance of concentrically laminated burrows from Lower Cretaceous bentonites, Oxfordshire. J. Geol. Soc. 153 (2), 255–263.

Gray, M.B., Nickelsen, R.P., 1989. Pedogenic slickensides, indicators of strain and deformation processes in redbed sequences of the Appalachian foreland. Geology 17 (1), 72–75.

Gulbranson, E.L., Sheldon, N.D., Montañez, I.P., Tabor, N.J., McIntosh, J.A., 2022. Late Permian soil-forming paleoenvironments on Gondwana: a review. Palaeogeogr. Palaeoclimatol. Palaeoecol. 586, 110762.

Gürel, A., 2017. Geology, mineralogy, and geochemistry of late Miocene paleosol and calcrete in the western part of the Central Anatolian Volcanic Province (CAVP), Turkey. Geoderm 302, 22–38.

Hembree, D.I., 2019. Burrows and ichnofabric produced by centipedes: modern and ancient examples. Palaios 34 (10), 468–489.

Hembree, D.I., Bowen, J.J., 2017. Paleosols and ichnofossil of the Upper Pennsylvanian-Lowe Monongahela and Dunkard Groups (OHIO, USA): a multi-proxy approach to unravelling complex variability in ancient terrestrial landscapes. Palaios 32 (5), 295–320.

Hetherington, A.J., Dolan, L., 2017. The evolution of lycopsid rooting structures: conservation and disparity. New Phytol. 215 (2), 538–544.

Huang, C., Retallack, G.J., Wang, C., 2012. Early Cretaceous atmospheric pCO2 levels recorded from pedogenic carbonates in China. Cretac. Res. 33 (1), 42–49.

Khademi, H., Mermut, A., 1999. Submicroscopy and stable isotope geochemistry of carbonates and associated palygorskite in Iranian Aridisols. Eur. J. Soil Sci. 50 (2), 207–216.

Khademi, H., Mermut, A., Krouse, H., 1997. Isotopic composition of gypsum hydration water in selected landforms from Central Iran. Chem. Geol. 138 (3–4), 245–255.

Klappa, C.F., 1980a. Brecciation textures and tepee structures in Quaternary calcrete (caliche) profiles from eastern Spain: the plant factor in their formation. Geol. J. 15 (2), 81–89.

Klappa, C.F., 1980b. Rhizoliths in terrestrial carbonates: classification, recognition, genesis and significance. Sedimentology 27 (6), 613–629.

Knaust, D., Bromley, R.G., 2012. Trace Fossils as Indicators of Sedimentary Environments, vol. 64. Elsevier.

Kraus, M.J., 1999. Paleosols in clastic sedimentary rocks: their geologic applications. Earth Sci. Rev. 47 (1), 41–70.

Kraus, M.J., Hasiotis, S.T., 2006. Significance of different modes of rhizolith preservation to interpreting paleoenvironmental and paleohydrologic settings: examples from Paleogene paleosols, Bighorn Basin, Wyoming, USA. J. Sediment. Res. 76 (4), 633–646.

Krull, E.S., Retallack, G.J., 2000. $\delta^{13}C$ depth profiles from paleosols across the Permian-Triassic boundary: evidence for methane release. Geol. Soc. Am. Bull. 112 (9), 1459–1472.

Löhr, S.C., Grigorescu, M., Cox, M.E., 2013. Iron nodules in ferric soils of the Fraser Coast, Australia: relicts of laterization or features of contemporary weathering and pedogenesis? Soil Res. 51, 77–93.
Loope, D.B., 2008. Life beneath the surfaces of active Jurassic dunes: burrows from the Entrada sandstone of south-Central Utah. Palaios 23 (6), 411–419.
Ludvigson, G.A., González, L., Fowle, D.A., Roberts, J.A., Driese, S.G., Villarreal, M.A., Smith, J., Suarez, M.B., Nordt, L., 2013. Paleoclimatic applications and modern process studies of pedogenic siderite. In: New Frontiers in Paleopedology and Terrestrial Paleoclimatology. SEPM (Society for Sedimentary Geology).
Machette, M.N., 1985. Calcic soils of the southwestern United States. Geol. Soc. Am. Spec. Pap. 203, 1–22.
Mack, G.H., James, W.C., Monger, H.C., 1993. Classification of paleosols. Geol. Soc. Am. Bull. 105 (2), 129–136.
Marriott, S., Wright, V., 1993. Palaeosols as indicators of geomorphic stability in two Old Red Sandstone alluvial suites, South Wales. J. Geol. Soc. Lond. 150 (6), 1109–1120.
Martindale, H., Van Der Raaij, R., Daughney, C.J., Morgenstern, U., Singh, R., Jha, N., Hadfield, J., 2019. Assessment of excess N_2 for quantifying actual denitrification in New Zealans groundwater systems. J. Hydrol. (NZ) 58 (1), 1–17.
Maynard, J., 1992. Chemistry of modern soils as a guide to interpreting Precambrian paleosols. J. Geol. 100 (3), 279–289.
McCarthy, P.J., Martini, I.P., Leckie, D.A., 1998. Use of micromorphology for palaeoenvironmental interpretation of complex alluvial palaeosols: an example from the Mill Creek Formation (Albian), southwestern Alberta, Canada. Palaeogeogr. Palaeoclimatol. Palaeoecol. 143 (1–3), 87–110.
Metzger, C.A., Retallack, G.J., 2010. Paleosol record of Neogene climate change in the Australian outback. Aust. J. Earth Sci. 57 (7), 871–885.
Mohammed, A.K., Hirmas, D.R., Nemes, A., Giménez, D., 2020. Exogenous and endogenous controls on the development of soil structure. Geoderma 357, 113945.
Mouraviev, F.A., Arefiev, M.P., Silantiev, V.V., Eskin, A.A., Kropotova, T.V., 2019. Paleosols and host rocks from the Middle-Upper Permian reference section of the Kazan Volga region, Russia: a case study. Palaeoworld 29 (2), 405–425.
Munsell, C., 2009. Munsell Soil Color Charts, (Revised Edition ed. Macbeth, Division of Kollmorgen Instruments Corp.
Myers, T.S., Tabor, N.J., Jacobs, L.L., Mateus, O., 2012. Estimating soil pCO2 using paleosol carbonates: implications for the relationship between primary productivity and faunal richness in ancient terrestrial ecosystems. Paleobiology 38 (4), 585–604.
Nordt, L., Atchley, S., Dworkin, S., 2003. Terrestrial evidence for two greenhouse events in the latest cretaceous. GSA Today 13 (12), 4–9.
Nordt, L., Driese, S.G., 2010. A modern soil characterization approach to reconstructing physical and chemical properties of paleo-Vertisols. Am. J. Sci. 310 (1), 37–64.
Nordt, L., Orosz, M., Driese, S.G., Tubbs, J., 2006. Vertisol carbonate properties in relation to mean annual precipitation: implications for paleoprecipitation estimates. J. Geol. 114 (4), 501–510.
Orr, T.J., Roberts, E.M., Wurster, C.M., Mtelela, C., Stevens, N.J., O'Connor, P.M., 2021. Paleoclimate and paleoenvironment reconstruction of paleosols spanning the Lower to Upper Cretaceous from the Rukwa Rift Basin, Tanzania. Palaeogeogr. Palaeoclimatol. Palaeoecol. 110539.
Orr, T.J., Wurster, C.M., Roberts, E.M., Singleton, R.E., Stevens, N.J., O'Connor, P.M., 2022. Paleoatmospheric CO_2 oscillations through a cool middle/Late Cretaceous recorded from pedogenic carbonates in Africa. Cretac. Res. 135, 105191.
Orr, T.J., Roberts, E.M., Bird, M.I., Mtelela, C., O'Connor, P.M., Stevens, N.J., 2023. Paleosol-derived paleoclimate and paleoenvironment reconstruction of the Rukwa Rift Basin, Tanzania: implications for faunal dispersal in the Miocene–Pliocene. J. Sediment. Res. 93 (5), 309–326.
Prochnow, S.J., Nordt, L.C., Atchley, S.C., Hudec, M.R., 2006. Multi-proxy paleosol evidence for middle and late Triassic climate trends in eastern Utah. Palaeogeogr. Palaeoclimatol. Palaeoecol. 232, 53–72.
Retallack, G.J., 1983. A paleopedological approach to the interpretation of terrestrial sedimentary rocks: the mid-Tertiary fossil soils of Badlands National Park, South Dakota. Geol. Soc. Am. Bull. 94 (7), 823–840.
Retallack, G.J., 1988. Field recognition of paleosols. Geol. Soc. Am. Spec. Pap. 216, 1–20.
Retallack, G.J., 1994. A pedotype approach to latest cretaceous and earliest Tertiary paleosols in eastern Montana. Geol. Soc. Am. Bull. 106 (11), 1377–1397.
Retallack, G.J., 1997. A colour guide to paleosols. John Wiley & Sons, Chichester, UK.
Retallack, G.J., 1998. Core concepts of paleopedology. Quat. Int. 51, 203–212.
Retallack, G.J., 2001. Soils of the Past: An Introduction to Paleopedology, 2nd ed. Blackwell Science.
Retallack, G.J., 2005. Pedogenic carbonate proxies for amount and seasonality of precipitation in paleosols. Geology 33 (4), 333–336.
Retallack, G.J., 2018. The oldest known paleosol profiles on Earth: 3.46Ga Panorama Formation, Western Australia. Palaeogeogr. Palaeoclimatol. Palaeoecol. 489, 230–248.
Retallack, G.J., Huang, C., 2010. Depth to gypsic horizon as a proxy for paleoprecipitation in paleosols of sedimentary environments. Geology 38 (5), 403–406.
Retallack, G.J., Noffke, N., 2019. Are there any ancient soils in the 3.7 Ga Isua Greenstone Belt, Greenland? Palaeogeogr. Palaeoclimatol. Palaeoecol. 514, 18–30.
Rochín-Bañaga, H., Gastaldo, R.A., David, D.W., Neveling, J., Kamo, S.L., Looy, C.V., Geissman, W.J., 2024. U-Pb dating of pedogenic calcite near the Permian-Triassic boundary, Karoo Basin, South Africa. Geol. Soc. Am. Bull. 136 (3–4), 1689–1700.
Sarjeant, W.A.S., 1975. Plant trace fossils. In: The Study of Trace Fossils. Springer, pp. 163–179.
Schaetzl, R.J., Thompson, M.L., 2015. Soils: Genesis and Geomorphology. Cambridge University Press.
Shearman, D., 1979. A field test for identification of gypsum in soils and sediments. Q. J. Eng. Geol. Hydrogeol. 12 (1), 51.
Sheldon, N.D., Tabor, N.J., 2009. Quantitative paleoenvironmental and paleoclimatic reconstruction using paleosols. Earth Sci. Rev. 95 (1), 1–52.
Tabor, N.J., Myers, T.S., 2015. Paleosols as indicators of paleoenvironment and paleoclimate. Annu. Rev. Earth Planet. Sci. 43, 333–361.
Tabor, N.J., Yapp, C.J., Montañez, I.P., 2004. Goethite, calcite, and organic matter from Permian and Triassic soils: carbon isotopes and CO2 concentrations. Geochim. Cosmochim. Acta 68 (7), 1503–1517.
Tabor, N., Myers, T., Michel, L., 2017. Sedimentologist's guide for recognition, description, and classification of paleosols. In: Terrestrial Depositional Systems. Elsevier, pp. 165–208.
Ufnar, D.F., González, L.A., Ludvigson, G.A., Brenner, R.L., Witzke, B.J., 2001. Stratigraphic implications of meteoric sphaerosiderite δ18O values in paleosols of the Cretaceous (Albian) Boulder Creek Formation, NE British Columbia foothills, Canada. J. Sediment. Res. 71 (6), 1017–1028.
Ufnar, D.F., Ludvigson, G.A., Gonzalez, L.A., Brenner, R.L., Witzke, B.J., 2004. High latitude meteoric delta O-18 compositions: Paleosol siderite in the Middle cretaceous Nanushuk Formation, North Slope, Alaska. Geol. Soc. Am. Bull. 116 (3–4), 463–473. https://doi.org/10.1130/b25289.1.
United States Department of Agriculture, 1971. Handbook of Soil Survey Investigations Field Procedures. USDA-SCS.
United States Department of Agriculture, 1975. Soil Taxonomy: A Basic System of Soil Classification for Making and Interpreting Soil Surveys. US Department of Agriculture.
United States Natural Resources Conservation, 1999. Soil Taxonomy: A Basic System of Soil Classification for Making and Interpreting Soil Surveys, 2nd ed. U.S. Dept. of Agriculture, Natural Resources Conservation Service.
United States Natural Resources Conservation, 2014. Soil Survey Staff: Keys to Soil Taxonomy. Natural Resources Conservation Service, Washington.
United States Natural Resources Conservation Service, 2014. Buried Soils and their Effect on Taxonomic Classification.
Valentine, T.A., Hallett, P.D., Binnie, K., Young, M.W., Squire, G.R., Hawes, C., Bengough, A.G., 2012. Soil strength and macropore volume limit root elongation rates in many UK agricultural soils. Ann. Bot. 110 (2), 259–270.
Vepraskas, M.J., 2004. Redoximorphic features for identifying aquic conditions: North Carolina Agricultural Research Service, Raleigh, North Carolina. Techn. Bull. 301, 33.
Wang, Y., Zheng, S.H., 1989. Paleosol nodules as Pleistocene paleoclimatic indicators, Luochuan, PR China. Palaeogeogr. Palaeoclimatol. Palaeoecol. 76 (1–2), 39–44.
Wang, Z., Rasbury, E., Hanson, G., Meyers, W., 1998. Using the U-Pb system of calcretes to date the time of sedimentation of clastic sedimentary rocks. Geochim. Cosmochim. Acta 62 (16), 2823–2835.
Weaver, J.E., 1968. Prairie Plants and their Environment. A fifty-year study in the midwest. Prairie plants and their environment. A fifty-year study in the midwest.
Wetzel, A., Carmona, N., Pnce, J., 2014. Tidal signature recorded in burrow fill. Sedimentology 61 (5), 1198–1210.
Whalley, W.R., Dumitru, E., Dexter, A.R., 1995. Biological effects of soil compaction. Soil Tillage Res. 35 (1), 53–68. https://doi.org/10.1016/0167-1987(95)00473-6.
Xiaoting, W., Mengying, Z., Yuehua, L., Ruixin, W., Xinqing, S., 2019. Covariation in root traits of Leymus chinensis in response to grazing in steppe rangeland. Rangeland J. 41 (4), 313–322.
Yaalon, D.H., Yaron, B., 1966. Framework for man-made soil changes – an outline of metapedogenesis. Soil Sci. 102 (4), 272–277.